Rechargeable Aluminum Batteries with Conducting Polymers as Positive Electrodes

Nicholas Stephen Hudak

Sandia National Laboratories

Rechargeable Aluminum Batteries with Conducting Polymers as Positive Electrodes

Nicholas S. Hudak
Advanced Power Sources Research & Development
Sandia National Laboratories
P.O. Box 5800 MS 0613
Albuquerque, New Mexico 87185-0613

Abstract

This report is a summary of research results from an Early Career LDRD project conducted from January 2012 to December 2013 at Sandia National Laboratories. Demonstrated here is the use of conducting polymers as active materials in the positive electrodes of rechargeable aluminum-based batteries operating at room temperature. The battery chemistry is based on chloroaluminate ionic liquid electrolytes, which allow reversible stripping and plating of aluminum metal at the negative electrode. Characterization of electrochemically synthesized polypyrrole films revealed doping of the polymers with chloroaluminate anions, which is a quasi-reversible reaction that facilitates battery cycling. Stable galvanostatic cycling of polypyrrole and polythiophene cells was demonstrated, with capacities at near-theoretical levels (30–100 mAh g^{-1}) and coulombic efficiencies approaching 100%. The energy density of a sealed sandwich-type cell with polythiophene at the positive electrode was estimated as 44 Wh kg^{-1}, which is competitive with state-of-the-art battery chemistries for grid-scale energy storage.

ACKNOWLEDGMENTS

CONTENTS

FIGURES

TABLES

NOMENCLATURE

Ah	ampere-hours
ATR	attenuated total reflectance
CHN	carbon-hydrogen-nitrogen
CIL	chloroaluminate ionic liquid
cm	centimeters
CV	cyclic voltammogram/voltammetry
Δf	change in frequency of QCM
Δm	change in mass on QCM surface
EMIC	1-ethyl-3-methylimidazolium chloride
EQCM	electrochemical quartz crystal microbalance
FTIR	Fourier transform infrared
g	grams
kg	kilograms
L	liter
LDRD	Laboratory Directed Research and Development
mAh	milliampere-hours
MCMB	mesocarbon microbeads
mg	milligram
OCP	open-circuit potential
PET	polyethylene terephthalate
PTFE	polytetrafluoroethylene
QCM	quartz crystal microbalance
SNL	Sandia National Laboratories
USGS	United States Geological Survey
Wh	watt-hours
wt%	weight percent

1. INTRODUCTION AND BACKGROUND

Demand for rechargeable battery systems continues to increase with the growth of the electric vehicle market[1] and the introduction of stationary energy storage to the electrical grid.[2] Rechargeable batteries based on aluminum are attractive alternatives to those based on conventional chemistries because of the high charge-storage capacity and relatively low cost of aluminum. The volumetric capacity of aluminum metal is 8.0 Ah cm^{-3}, which is four times higher than that of lithium. Aluminum is also competitive in terms of gravimetric capacity (3.0 Ah g^{-1} vs. lithium's 3.9 Ah g^{-1} or sodium's 1.2 Ah g^{-1}). Aluminum is the most abundant metal in the earth's crust, and its cost is significantly lower than that of most other metals used for electrochemical energy storage. This makes aluminum-based batteries particularly attractive for stationary energy storage, the large scale of which requires the use of inexpensive raw materials.[3] According to the US Geological Survey, worldwide production of aluminum (by weight) in 2010 was 1600 times that of lithium.[4] Although domestic lithium production is not disclosed by USGS, they do report that the net reliance on imports of lithium in 2006-2009 (as a percentage of consumption) was greater than 50%.[4] Over the same time period, the net reliance on imports of aluminum ranged from 0-38%. Thus, the domestic availability of aluminum makes it a much less expensive raw material than lithium, and this may have implications for battery production as demand increases.

Historically, aluminum batteries based on aqueous or high-temperature molten salt electrolytes have been the subject of extensive research but have not been considered for commercialization because of prohibitive technical barriers.[5] An alternative type of rechargeable aluminum battery is based on room-temperature ionic liquids comprising imidazolium salts and aluminum chloride (i.e. chloroaluminate ionic liquids, or CILs). Aluminum metal can be electrochemically plated and stripped with high efficiency (98.6–99.8% coulombic efficiency) at room temperature in such electrolytes,[6-9] and these reactions form the basis for the negative electrode (anode) in a rechargeable aluminum-metal battery. Both aluminum metal and CIL electrolytes are non-flammable, so a battery based on these components would have significant safety advantages over conventional lithium- and sodium-based batteries. Furthermore, the conductivities of imidazolium-based CILs[7, 10] are on par with those of lithium-ion battery electrolytes.[11]

The main obstacle to development of a rechargeable aluminum battery based on CIL electrolytes is the identification of an active charge-storage material for the positive electrode (cathode). While the electrochemical plating and stripping of aluminum metal in CILs have been studied in great detail,[6-9, 12, 13] there have been far fewer demonstrations of active cathode materials for CIL-based batteries. One early demonstration of a rechargeable aluminum-metal cell used graphite as the active material at the positive electrode with a mixture of aluminum chloride ($AlCl_3$) and 1,2-dimethyl-3-propylimidazolium chloride as the electrolyte.[14] The proposed reaction at the positive electrode was the reversible intercalation and removal of Cl_2 from the graphite, but the presence of molecular chlorine in the graphite was not confirmed. A relatively flat cell potential around 1.7 V was observed, and the maximum charge-storage capacity was 35 mAh g^{-1} relative to the mass of graphite. This capacity rapidly decreased with cycling, which was attributed to disintegration of the graphite electrode. Another demonstration with a similar electrolyte utilized metal halides as active cathode materials.[15] During cell discharge, the metal halides presumably converted to aluminum halides. While some cycling of the cells was demonstrated, a significant amount of self-discharge occurred as a result of metal halide dissolution in

the electrolyte. More recently, there have been reports of "aluminum-ion" cathodes using MnO_2,[16] V_2O_5,[17] or fluorinated graphite[18] as Al(III)-insertion hosts in CIL electrolytes. However, evidence of an aluminum-intercalated phase was not given in any of these cases. Subsequently, electrochemical activity and apparent capacity at the cathode of the V_2O_5/Al cell were wholly attributed to a reaction between the CIL and the stainless steel current collector.[19] Given the great difficulties encountered in developing cathode materials that can reversibly insert divalent magnesium ions,[20] it is likely that the identification of a host for reversible insertion of trivalent aluminum will be an even greater challenge.

Perhaps the most promising active materials for positive electrodes in CIL-based aluminum batteries are conducting polymers. Such polymers can be electrochemically oxidized and reduced in electrolyte solutions, so they have been extensively researched as electrode materials for lithium-ion batteries.[21] Concurrent with electro-oxidation, the conducting polymer changes from neutrally-charged to positively-charged and is doped with anions from the electrolyte to maintain electro-neutrality. Upon electro-reduction of the polymer, the anions are transferred back to solution. The use of conducting polymers as anion-insertion electrodes in aluminum-based electrolytes has been demonstrated only a few times. Osteryoung and co-workers first demonstrated the electrochemical activity of polypyrrole,[22] polythiophene,[23] polyaniline,[24] and poly(p-phenylene)[25] electrodes in mixtures of $AlCl_3$ and 1-ethyl-3-methylimidazolium chloride ($AlCl_3$:EMIC, one of the most common CILs) at room temperature. The polymers had been synthesized via electropolymerization in solutions containing the corresponding monomer and $AlCl_3$:EMIC. Electrode characterization in these studies focused on cyclic voltammetry. Metrics that are important for battery characterization (such as specific capacity, coulombic efficiency, and cycling stability) were not reported. Only Koura and co-workers, in several demonstrations with polyaniline and poly(p-phenylene) electrodes in CIL-aluminum cells, reported a very limited amount of data on galvanostatic cycling, specific capacity, and self-discharge behavior.[26-30]

Presented here is an examination of the use of polypyrrole and polythiophene as positive electrodes in aluminum battery cells with chloroaluminate ionic liquid electrolyte. Distinct from previous studies of conducting polymers in aluminum cells, characterization is focused on battery-relevant metrics, including gravimetric capacity, gravimetric energy density, coulombic efficiency, potential profile, cycling stability, and rate capability. Polymer electrodes in two different forms were examined: (1) electrochemically polymerized films in flooded, three-electrode cells and (2) composite electrodes made of commercially-available conducting polymers and binder in sealed sandwich-type cells. The relevant electrode reactions were identified and investigated using chemical and electrochemical analysis of the conducting polymer films. Cycling of the polymer electrodes was performed in $AlCl_3$:EMIC electrolyte with concomitant stripping and plating of aluminum metal at the counter electrode. The results give a quantitative performance evaluation of conducting polymers as active cathode materials for rechargeable aluminum batteries operating at room temperature.

2. EXPERIMENTAL METHODS

Anhydrous aluminum chloride and the chloroaluminate ionic liquids are extremely sensitive to air and moisture. All chemical handling and cell preparation were performed in an argon-filled glove box (oxygen and water content < 1ppm) unless otherwise specified. Electrochemical cells (except for the sealed Swagelok®-type cells) remained in the glove box during electrochemical testing.

2.1. Chemicals

Pyrrole, thiophene, polypyrrole powder, and poly(thiophene-2,5-diyl) powder were used as received from Sigma-Aldrich. Aluminum chloride (99.999%, ultra dry), 1-ethyl-3-methylimidazolium chloride (98+%), SP carbon black, aluminum foil (various thicknesses, 99.99%), and aluminum wire (1.0 mm diameter, 99.99%) were used as received from Alfa Aesar. Acetonitrile (99.9%, extra dry), acetone (99.8%, extra dry), dibutyl pthlalate (99%), and diethyl ether (99.5%, extra dry) were used as received from Fisher Scientific (Acros Organics). Kynar Flex® 2801 (hexafluoropropylene-vinylidene fluoride copolymer) was used as received from Arkema.

AlCl$_3$:EMIC mixtures were prepared by slowly adding appropriate amounts of aluminum chloride to 1-ethyl-3-methylimidazolium chloride and mixing with a magnetic stir bar. AlCl$_3$:EMIC mixtures with a molar ratio greater than 1:1 were purified as follows with an electrochemical stripping/plating procedure similar to the electrolysis procedure employed by Tierney et al.[31] A two-electrode cell was assembled by immersing two pieces of aluminum foil (2-3 cm^2 each) into the mixture. Continuous plating onto the working electrode was performed at room temperature by galvanostatic hold (−5 or −10 mA) with a Princeton Applied Research 263A potentiostat/galvanostat. This current was applied until a transparent, light-yellow-to-colorless solution resulted and no further visible changes occurred (2–3 days). Fresh aluminum electrodes were introduced into the solution as necessary during this time period.

2.2. Electrochemical Polymerization and Characterization

Polymerization of pyrrole and thiophene on electrode surfaces was performed electrochemically at room temperature as follows. The polymerization solution consisted of 0.3 mole L^{-1} pyrrole or thiophene in AlCl$_3$:EMIC (1:1 molar ratio),[22, 23, 32] which was prepared by stirring the monomer in AlCl$_3$:EMIC for several minutes. The working electrode in the three-electrode cell had a circular exposed area and was made of glassy carbon (3-mm diameter, Bioanalytical Sciences) or stainless steel 316 (7/16-inch diameter). The counter and quasi-reference electrodes were made of aluminum wire. The three electrodes were suspended in the polymerization solution in a glass vial. Galvanostatic polarization was performed at +1 mA cm^{-2} (oxidative current density relative to the working electrode area) for a specified amount of time using a Princeton Applied Research 263A potentiostat/galvanostat. Following this step, the resultant polymer-coated electrode was rinsed by dipping it in acetonitrile, which was then allowed to evaporate.

Electropolymerized films on glassy carbon were used for further electrochemical characterization at room temperature in three-electrode cells. The same three-electrode cell configuration in the glove box was used, but in this case the electrolyte was pure AlCl$_3$:EMIC (1.5:1 molar

11

ratio). The counter and quasi-reference electrodes were made of aluminum wire. Electrochemical experiments, including cyclic voltammetry and galvanostatic cycling, were performed with a Princeton Applied Research 263A potentiostat/galvanostat.

2.3. Electrochemical Quartz Crystal Microbalance (EQCM)

Electrochemical polymerizations of pyrrole and thiophene were also performed on an EQCM at room temperature using a Princeton Applied Research QCM922 instrument with a well-cell resonator holder. The platinum resonator also acted as the working electrode for electropolymerization, and aluminum wires were placed in the cell as counter and reference electrodes. For each experiment, an aliquot of 250-300 µL of polymerization solution was added to the well immediately prior to electropolymerization. Electrochemical polymerization was performed galvanostatically at +1 mA cm^{-2} for 400 seconds, as described in the previous section. The resonant frequency of the resonator was monitored and recorded before, during, and after this polymerization step. The Sauerbrey Equation[33] was used to convert changes in resonant frequency to changes in mass.

2.4. Chemical Characterization

Electropolymerized polypyrrole films that peeled easily off the stainless steel substrate were transferred under argon to a dry room, where they were weighed on a laboratory balance with 10-µg resolution. Fourier transform infrared (FTIR) spectra of electropolymerized polypyrrole films were recorded on a Thermo Nicolet iS10 FTIR equipped with a Smart Orbit (Diamond) ATR (attenuated total reflectance) accessory, all of which were also located in the dry room. The dew point of the dry room was maintained at less than −40°C. Other samples of peeled-off, electropolymerized polypyrrole films were packaged under argon and sent to ALS Life Sciences in Tucson, AZ for elemental analysis, which included micro CHN analysis, ion chromatography with an oxygen flask, and inductively couple plasma.

2.5. Electrode Tape Fabrication

Free-standing composite electrodes (called "tapes") with polypyrrole, polythiophene, or mesocarbon microbeads (MCMB) as active materials were fabricated in the dry room (<−40°C dew point) using the Bellcore method[34] as follows. Polypyrrole, polythiophene, or MCMB powder was mixed with Kynar Flex® 2801 (as binder), SP Carbon Black (as conductive additive), and dibutyl phthalate (as plasticizer) in a small vial with the approximate weight ratio 6:3:1:3. An excess of acetone was added to the vial, and the suspension was stirred with a magnetic stir bar until a smooth consistency was formed (30 minutes for polythiophene, 48 hours for polypyrrole, and 90 minutes for MCMB suspensions). The suspension was cast onto a moisture-resistant polyester (polyethylene terephthalate, or PET) film with a doctor blade, and the acetone was allowed to evaporate. The resultant electrode-tape was passed through a laminator at 130°C, and dibutyl phthalate was extracted from the tape by immersing it in diethyl ether three times for fifteen minutes each time. The weight-percent of active material in the resultant film was calculated by the mass of powders added to the original mixture (approximately 60 wt% in each case). Discs with 6-mm diameter were punched from the electrode tapes, weighed on a laboratory bal-

ance having 10-µg resolution, and transferred in a dry container from the dry room to the glove box.

2.6. Assembly and Testing of Sandwich-Type Cells

Custom-made Swagelok® cell fixtures consisted of a polytetrafluoroethylene (PTFE) body (6-mm diameter channel), glassy carbon rod as cathode current collector, and copper disc as anode current collector. A copper rod (alloy 110) and copper-plated spring were also used at the anode to compress the cell components. The separators were Whatman® GF/D glass micro-fiber mats (0.67 mm dry thickness). Cells were assembled in the glove box by stacking the cathode-tape disc, one separator disc soaked in $AlCl_3$:EMIC (1.5:1 molar ratio), and one aluminum disc in the fixture. Cells were sealed and removed from the glove box for testing. Galvanostatic cycling of the cells was performed on an Arbin BT-2043 multichannel battery cycler with the cells in a temperature chamber maintained at 30°C.

3. RESULTS AND DISCUSSION

3.1. Electrochemical Polymerization

Both pyrrole and thiophene were electrochemically polymerized with the chloroaluminate ionic liquid $AlCl_3$:EMIC as electrolyte. This allowed fast and simple preparation of polypyrrole and polythiophene, to be tested as active materials for the positive electrode (cathode) in rechargeable aluminum battery cells. Typically, oxidative electropolymerization produces a cationic conducting polymer and is accompanied by "doping" with anions from the electrolyte solution to maintain electro-neutrality.[21] In the work presented here, electropolymerization was performed in the same electrolyte as the cycling aluminum batteries to prevent contamination and unwanted side reactions and to ensure that the polymer was doped with compatible chloroaluminate anions. Galvanostatic polarization was used for the polymerization to allow systematic variation of the amount of polymer deposited and to ensure that a repeatable amount of polymer was deposited. This is distinct from previous demonstrations of electropolymerization in CIL electrolytes, in which potentiostatic polarization was used.[22, 23, 32]

For the electropolymerization on glassy carbon substrates, a current density of 1 mA cm^{-2} and polymerization time of 400 seconds were used. For both monomers, this electrochemical polymerization produced a dull black film on the electrode surface. The applied current density

Figure 1. Galvanostatic polymerization of pyrrole in $AlCl_3$:EMIC (1:1 molar ratio) at room temperature. **(a)** Current density vs. time. **(b)** Potential vs. time for cells with glassy carbon electrode (dashed line) and platinum/EQCM electrode (solid line). **(c)** Resonant frequency of EQCM electrode vs. time.

15

and resultant potential vs. time are shown in Figures 1 and 2 for pyrrole and thiophene, respectively. Galvanostatic polarization produces an immediate jump in potential in both cases. As shown in Figure 1(b), polymerization of pyrrole on glassy carbon or platinum occurred around 1.4 V vs. Al (all potentials quoted here are relative to the aluminum metal quasi-reference electrode in the same electrolyte as the given cell). This potential is significantly more oxidizing than the applied potential in previous demonstrations of pyrrole polymerization in CILs.[22, 32] Thus, the applied current density produced a potential that should be sufficient for polymerization. Similarly, electro-oxidation of thiophene at 1 mA cm^{-2} occurred above 1.8 V, as shown in Figure 2(b), and this should be sufficiently oxidizing to induce polymerization.

The same electropolymerization protocol (1 mA cm^{-2} for 400 seconds) was used in EQCM cells in which the working electrode was made of platinum. As shown in Figures 1(b) and 2(b), the potential response from galvanostatic polymerization for both monomers was similar in glassy carbon and EQCM cells. Slight differences in potential between the two types of cells may be simply due to a difference in ohmic drop considering that the cell geometries (flooded vial cell vs. EQCM well-shaped cell) are quite different. Thus, it is presumed that quantitatively similar polymerization occurred on glassy carbon and platinum substrates. For the EQCM cell, the platinum working electrode also acts as the resonator, which is sensitive to the presence of added mass. The resonant frequency of this electrode vs. time during electropolymerization is shown in Figures 1(c) and 2(c) for pyrrole and thiophene, respectively. For pyrrole polymerization, a linear decrease in resonant frequency was observed for the period of time in
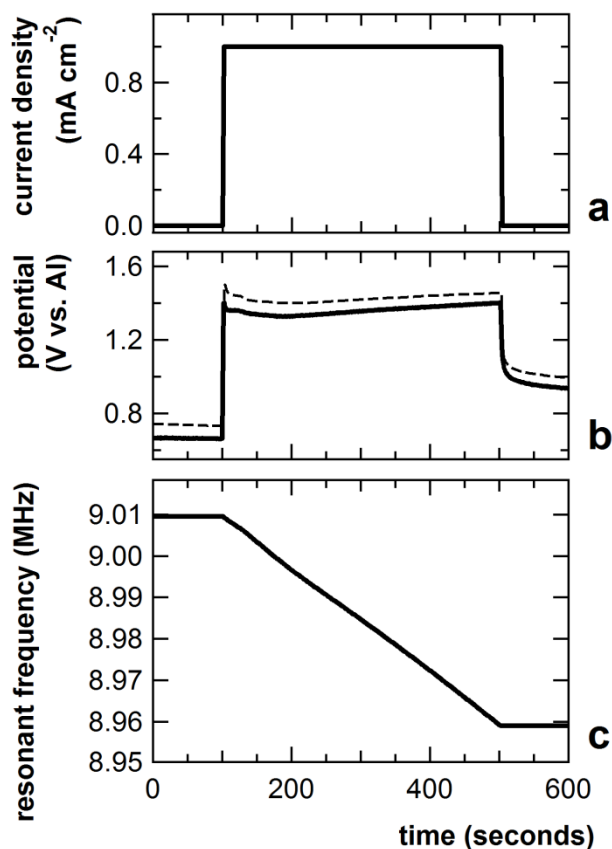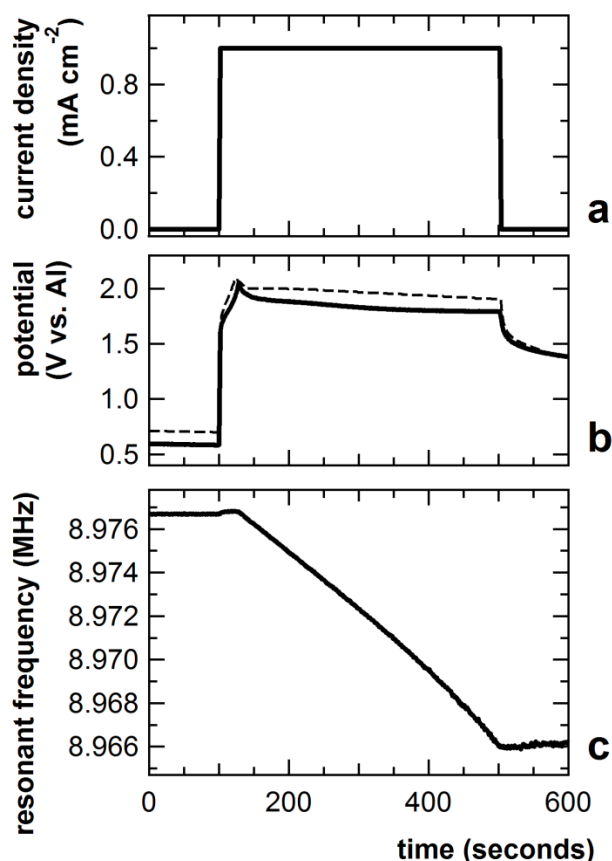

Figure 2. Galvanostatic polymerization of thiophene in AlCl$_3$:EMIC (1:1 molar ratio) at room temperature. **(a)** Current density vs. time. **(b)** Potential vs. time for cells with glassy carbon electrode (dashed line) and platinum/EQCM electrode (solid line). **(c)** Resonant frequency of EQCM electrode vs. time.

16

which the constant current density was applied. For thiophene polymerization, the first ~50 seconds of galvanostatic polarization produced no change in resonant frequency while the potential gradually increased. After a maximum in potential was reached, the potential gradually decreased and the resonant frequency decreased in a roughly linear way. The ~50-second initiation period may be a non-faradaic process in which no polymerization occurs while the potential is increased to a value sufficiently oxidizing for polymerization. The steady decrease in resonant frequency after this initiation period suggests that the remainder of the polarization results in continued polymerization with the polymer being deposited on the electrode surface.

The linearity of the QCM frequency response for both monomers in the range examined is strong evidence that the deposited polymer films act as rigid layers.[35] Any amount of swelling in such a "rigid-layer" film with liquid from the electrolyte is not sufficient to produce viscoelastic behavior; the absence of viscoelastic behavior allows use of the Sauerbrey Equation to relate changes in frequency (Δf) to changes in mass (Δm).[33] Thus, the changes in frequency observed for pyrrole and thiophene polymerizations were used to calculate the masses of polymer deposited. EQCM polymerizations of pyrrole and thiophene were each performed in quadruplicate, and the average and standard deviation values are shown in Table 1. The *in situ* Δf values were calculated by taking the stable frequency values, with electrolyte present in the cell, before and after the 400-second polymerization period. The Δm values, also shown in Table 1, were calculated using the Sauerbrey Equation and normalized to electrode area. Because the EQCM electrode surface was initially bare, the normalized Δm values correspond to the total amount of polymer on the electrode. These values will be used below to estimate the gravimetric charge-storage capacity of the conducting polymers in CIL electrolytes. As further confirmation of rigid-layer behavior, *ex situ* Δf and Δm values were also calculated by measuring the resonant frequency values before and after polymerization in the absence of electrolyte solution. After polymerization, the electrode was rinsed in acetonitrile. The excess acetonitrile was removed, and the resonant frequency of the electrolyte-free electrode was immediately measured. The close agreement between *in situ* and *ex situ* Δf values is further confirmation that the presence of electrolyte liquid has a negligible effect on the measurement of polymer film mass using QCM.

Table 1. EQCM Results for Electrochemical Polymerization. *In situ* and *ex situ* frequencies were measured in the presence and absence, respectively, of liquid electrolyte. Each number is the average ± standard deviation of four separately prepared cells.

	Δf (kHz)	Δm (μg)	Δm/area (mg/cm^2)
polypyrrole *in situ*	50.7 ± 1.4	54.4 ± 1.6	0.277 ± 0.008
polypyrrole *ex situ*	49.7 ± 2.9	53.2 ± 3.2	0.271 ± 0.016
polythiophene *in situ*	10.5 ± 2.8	11.2 ± 3.0	0.0573 ± 0.0154
polythiophene *ex situ*	10.6 ± 2.5	11.4 ± 2.6	0.0580 ± 0.0135

3.2. Characterization of Electropolymerized Polypyrrole Films

Electrochemical polymerization of thicker polypyrrole films on stainless steel produced cohesive, black films that easily peeled off the substrate after rinsing in acetonitrile. These free-standing polypyrrole films were used for further characterization because they were easy to transport and handle. The FTIR spectrum of such a polypyrrole film (1 mA cm^{-2} polymerization for 1000 seconds) is shown in Figure 3. The seven prominent FTIR peaks in Figure 3 closely match those of previously published spectra for polypyrrole doped with ClO_4^- or AsF_6^-.[36] The wavenumbers of these peaks are given in Table 2 along with the corresponding wavenumbers of an undoped polypyrrole sample from the same reference. Also given in Table 2 are the assignments for five of the peaks as described by Tian and Zerbi.[37] The wavenumbers of the peaks for the sample synthesized here match those of the doped sample much more closely than those of the undoped sample. This is strong evidence that the galvanostatic polymerization of pyrrole in CIL electrolyte produced doped polypyrrole. Such identification was assumed in previous studies of polypyrrole synthesis in CIL electrolyte but was not confirmed.[22, 32]
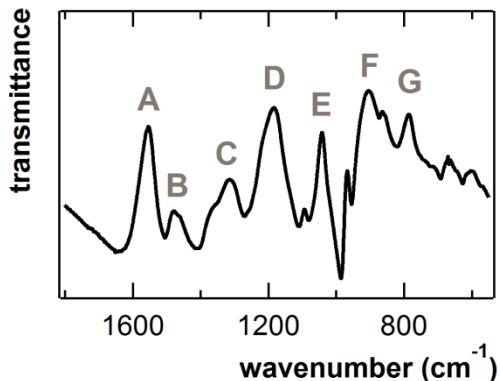
Figure 3. FTIR-ATR spectrum of free-standing polypyrrole film, synthesized by galvanostatic polymerization at 1 mA cm^{-2} for 1000 seconds in a solution of 0.3 M pyrrole in 1:1 AlCl$_3$:EMIC at room temperature.

Table 2. Peaks from FTIR spectrum of Figure 3 compared to those reported[36] for doped and undoped polypyrrole. Peak assignments as previously identified.[37]

Peak	Approximate assignment[37]	Observed wavenumber (cm^{-1})	Reported (doped with ClO_4^-)[36] (cm^{-1})	Reported (undoped)[36] (cm^{-1})
A	C-C & C=C stretch	1550	1550	1530
B	C-N stretch	1480	1470	1440
C	C-H & N-H deformation	1310	1300	1300
D	C-N stretch & C-H def.	1180	1180	1240
E	C-H deformation	1040	1000	1050
F	unidentified	910	900	960
G	unidentified	790	780	750

Thicker polypyrrole films that peeled off the substrate were also weighed with a laboratory balance for comparison with QCM-measured mass. The mass was varied by varying the polymerization time at 1 mA cm^{-2}. Shown in Figure 4 are the resultant mass values as a function of the total applied charge during polymerization. At lower values of applied charge, a linear relationship between the two values was observed because the amount of polymer mass created was proportional to the amount of charge applied during polymerization. This is similar to the EQCM observation in which resonant frequency linearly decreased with polymerization time. A least-squares linear fit of the four data points with mass less than 1.5 mg in Figure 4 produces a slope of 2.64 mg mAh^{-1}. For comparison to EQCM measurements, this value is multiplied by the area-specific amount of charge applied in EQCM experiments (0.111 mAh cm^{-2}) to obtain a value of 0.293 mg cm^{-2}. This value is close to the mass loading calculated with the Sauerbrey Equation and given in Table 1. This is further confirmation of the validity of the EQCM-Sauerbrey method described above. As thicker films are polymerized, the amount of mass deposited per unit charge tends to decrease, as shown in Figure 4. This may be due to less efficient polymerization or lower amounts of doping in thicker films.
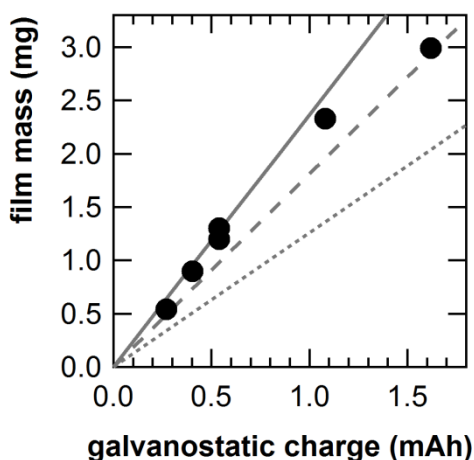
Figure 4. Mass of polypyrrole films (markers) as a function of charge applied during electropolymerization at 1 mA cm^{-2}. Mass measured with laboratory balance. Theoretical values (lines) calculated assuming a dopant level of one anion per four monomers. Assumed dopant in calculation is $Al_2Cl_7^-$ (solid line), $AlCl_4^-$ (dashed line), or Cl^- (dotted line).

The film mass data in Figure 4 is also useful for estimating the amount and type of doping that occurs in the polymerization process in CIL electrolyte. The electrochemical synthesis of polypyrrole has been well documented using other electrolyte media and a variety of anion dopants such as ClO_4^-, BF_4^-, and PF_6^-.[38] In the case of $AlCl_3$:EMIC with a molar ratio 1:1, the main anionic component is $AlCl_4^-$ because the $AlCl_3$ molecules form complexes with the Cl^- ions from EMIC. However, $AlCl_4^-$ can dissociate into $Al_2Cl_7^-$ and Cl^-, so all three anions are present to some extent in the solution.[7, 39] Assuming the polymer becomes doped with one of these ions during electropolymerization, theoretical values can be calculated as follows for the synthesized polymer mass (i.e. mg mAh^{-1} with respect to applied polymerization charge). The doping amount after polymerization and with subsequent cycling is 3 to 4 pyrrole monomers per anion equivalent and is largely independent of the anion used.[38] During oxidative polymerization, the total amount of charge consumed is two equivalents per monomer plus one equivalent per monovalent anion molecule. The calculated theoretical values are shown as lines in Figure 4 for each of the three anions, assuming a dopant level of one anion per four monomer units (25%

doping). As is evident in Figure 4, the experimental data lies between the theoretical values for doping with $AlCl_4^-$ and $Al_2Cl_7^-$. Thus, the polypyrrole films that are electrochemically synthesized in CIL electrolytes are doped with chloroaluminate anions and not with Cl^-. Even if the doping level was an unprecedented one anion per monomer unit, polypyrrole doped with Cl^- could not result in the masses observed here.

Elemental analysis was performed on electrochemically synthesized films to obtain a better estimate of the dopant level and identity. Repeated polymerization experiments at 1 mA cm^{-2} for 50-100 minutes on stainless steel substrates (0.97 cm^2) were performed until a total of ~40 mg of sample was obtained. The results, in mass-percent and mole-percent, are shown in Table 3. The presence of aluminum and chlorine confirms that the dopants are chloroaluminate anions. The molar ratio of chlorine to aluminum is 3.82, indicating that the polymer film consists of 77.7 mol% $AlCl_4^-$ dopant and 22.3 mol% $Al_2Cl_7^-$ dopant. The ratios of Al and Cl to N can be used to calculate a dopant level of 24.6%, or one anion equivalent per four pyrrole monomers. This is the first known measurement of dopant level in a polypyrrole-chloroaluminate material, and it is in close agreement with dopant levels in other forms of polypyrrole.[38] Considering that the samples used for this elemental analysis ranged from 2–3 mg, this measured dopant level is in agreement with the data in Figure 4, which shows that a mixture of $AlCl_4^-$ and $Al_2Cl_7^-$ must be present if the dopant level is 25%. Thicker films probably tend toward a larger proportion of $AlCl_4^-$ due to a depletion of $AlCl_3$ in the polymerization solution with continued reaction. Thinner films, such as those fabricated in EQCM experiments here, may tend toward a higher proportion of $Al_2Cl_7^-$. However, this could not be confirmed because the observations in Figure 4 may also be due to higher dopant levels in thinner films.

Table 3. Elemental analysis results for electrochemically synthesized polypyrrole films.

	mass%	mole%	moles per mole of N
carbon	39.54	36.6	3.92
hydrogen	3.67	40.5	4.34
nitrogen	11.76	9.34	1.00
chlorine	34.21	10.7	1.15
aluminum	6.82	2.81	0.301

3.3. Proposed Electrode Reactions

In the aluminum battery cell proposed here, the reversible reaction at the negative electrode is the well-known stripping and deposition of aluminum metal with CIL electrolytes:[6-9]

$$Al + 7AlCl_4^- \leftrightarrow 4Al_2Cl_7^- + 3e^- \hspace{2cm} (1)$$

The cationic species in the electrolyte does not participate in the reaction. The $Al_2Cl_7^-$ anion is a complex of two $AlCl_3$ molecules and one Cl^- ion. Aluminum can only be electrodeposited when $Al_2Cl_7^-$ is present. In the case of $AlCl_3$:EMIC, $Al_2Cl_7^-$ is present when there are more moles of

AlCl$_3$ than EMIC (also known as an acidic solution). Thus, the electrolyte must be maintained in an acidic condition; i.e. the molar ratio of AlCl$_3$ to EMIC must be greater than one.

Given the conclusion from the preceding section that the conducting polymers are doped with chloroaluminate anions from the electrolyte, the following reaction is proposed for the positive electrode (cathode):

$$3(X^+\,AlCl_4^{\,-}) + 3e^- \leftrightarrow 3X + 3AlCl_4^{\,-} \tag{2}$$
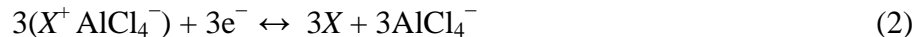
where X is an arbitrary host for cations, which alternates between being positively charged or neutral. X can be any number of monomers in a conducting polymer or can be another oxidizable host for anions, such as graphite.[40, 41]

The full cell reaction is the sum of the positive and negative electrode reactions (cell discharge from left to right):

$$Al + 4AlCl_4^{\,-} + 3(X^+\,AlCl_4^{\,-}) \leftrightarrow 4Al_2Cl_7^{\,-} + 3X \tag{3}$$

The only anions in the fully charged cell are AlCl$_4^{\,-}$ anions, and the only anions in the fully discharged cell are Al$_2$Cl$_7^{\,-}$. Thus, the composition of the electrolyte (i.e. its acidity) changes with state-of-charge. At intermediate states-of-charge, the cathode host may be doped with a mixture of the two chloroaluminate anions, as was shown in the preceding section. There are no free Cl$^-$ ions in the cell reaction, as this would be mean the electrolyte is in a basic condition and unable to electrodeposit aluminum metal at the negative electrode.

The combination of metal anode and anion-insertion cathode in the full cell reaction results in a cycling mechanism that is distinct from "rocking chair" batteries such as lithium-ion batteries. The cycling mechanism proposed here relies on the participation of electrolyte anions, and the amount of freely mobile in the liquid electrolyte changes with state-of-charge. As shown in Equation 4, the electrolyte anions do not cancel out of the full cell reaction. The amount of electrolyte must be scaled with the amount of cathode material X. As such, estimations of gravimetric or volumetric energy density must account for the amount of electrolyte present in addition to the amount of electrode material. An upper bound for theoretical gravimetric charge-storage capacity can be calculated by using the full cell reaction and incorporating cations such as 1-ethyl-3-methylimidazolium (EMI):

$$Al + 4(EMI^+\,AlCl_4^{\,-}) + 3(X^+\,AlCl_4^{\,-}) \leftrightarrow 4(EMI^+\,Al_2Cl_7^{\,-}) + 3X \tag{4}$$
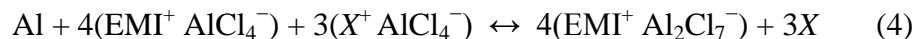
The cations must be present to balance the charge of anions, so they are included in the calculation of gravimetric capacity. Using the right side of Equation 4, the molecular weights of 4EMI, 4Al$_2$Cl$_7^{\,-}$, and 3X are used with a three-electron transfer to calculate gravimetric capacity. An upper bound for capacity is calculated by considering a weightless cathode host (i.e. molecular weight of X equals zero), and the resultant value is 48.6 mAh g^{-1}. If X is equivalent to four pyrrole monomers, as was observed experimentally in the previous section, the capacity is 32.7 mAh g^{-1}. If X is equivalent to four thiophene monomers, the capacity is 30.2 mAh g^{-1}. These capacity values are specific to the total mass of all active cell components, including the CIL electrolyte and aluminum metal anode. For a cell with a nominal voltage of 1.6 V, the theoretical energy density would range from 48 to 78 Wh kg^{-1}. Using this strategy, the electrode-specific capacities measured in the following sections will be used to estimate cell-specific energy densities.

3.4. Electrochemical Characterization of Conducting Polymer Films

Films of polypyrrole and polythiophene that were electrochemically synthesized on glassy carbon substrates underwent electrochemical characterization in three-electrode cells. The electrolyte used for characterization was $AlCl_3$:EMIC with a 1.5:1 molar ratio (an acidic composition). This CIL has an approximately equimolar amount of $AlCl_4^-$ and $Al_2Cl_7^-$ and thus would be the composition at which the proposed battery cell is at 50% state-of-charge. This is also more appropriate for a battery-related study than the neutral and basic CIL electrolyte used in previous studies of polypyrrole[22, 32] and polythiophene.[23] The neutral and basic compositions contain only negligible amounts of $Al_2Cl_7^-$, so they do not allow the reversible plating and stripping of aluminum metal that is required for a rechargeable battery.

Cyclic voltammograms (CV) of both polymer films were recorded at room temperature with 1.5:1 $AlCl_3$:EMIC electrolyte. Prior to the CV experiments, the electrodes were removed from the polymerization solution, rinsed in acetonitrile, immersed in pure 1.5:1 $AlCl_3$:EMIC, and allowed to rest at open circuit for one hour. CV curves recorded at 10 mV s^{-1} over the range 0.1–2 V vs. Al are shown in Figure 5 (dashed lines) and compared to the same CV of a bare glassy carbon electrode (bold solid line). Polypyrrode and polythiophene films exhibited significant electrochemical activity compared to the bare electrode. Faradaic redox processes (exhibited by peak-pairs) and non-faradaic activity (exhibited by broad current-potential curves) were both observed in both polymers. The faradaic redox process in each polymer is presumably the anion-doping reaction described above. The non-faradaic activity is due to double-layer charging (capacitance) at the polymer surface, which may proceed via mechanism similar to anion-doping. For both polymers, non-faradaic activity was only observed at potentials more positive (oxidizing) than the redox potential of the faradaic process. This is because a conducting polymer is insulating below the redox potential, i.e. in its neutrally-charged form. Non-faradaic cycling is only possible at potentials above the redox potential, when the polymer is in its oxidized, conducting, doped form.

The CV curves in Figure 5 are qualitatively similar to previously published curves;[22, 23] any difference in shape and redox potential could simply due to a difference in polymerization procedure or electrolyte composition. The broad shape of the redox peaks prevents a precise determination of redox potential. However, Figure 5 shows that the redox potential of polythiophene was about one volt higher than that of polypyrrole, which is in agreement with previous observations in other electrolytes.[38] This also suggests that polythiophene is a better candidate for application in aluminum batteries, which require as high a voltage as possible to achieve high energy density.

Although the curves in Figure 5 have no resemblance to a classically reversible CV shape, the amount of charge transferred during oxidation was approximately equal to that transferred during reduction over the potential range 0.1–2 V. When the potential range was extended to 0.1–2.6 V, as shown in Figure 6, additional redox processes occurred at higher potentials. These processes were highly irreversible as the amount of charge transferred during oxidation was significantly higher than that transferred during reduction. As shown in Figure 6, such irreversible processes also occurred to a significant extent on the bare glassy carbon electron. Thus, they can be attributed to reactions arising mainly from the CIL electrolyte. This was previously observed with 1.5:1$AlCl_3$:EMIC on tungsten electrodes and was attributed to chlorine evolution from $AlCl_4^-$.[42] In both the previous report on tungsten electrodes and the present report on glassy carbon electrodes, the irreversible reaction or reactions occurred above 1.5 V and, to a
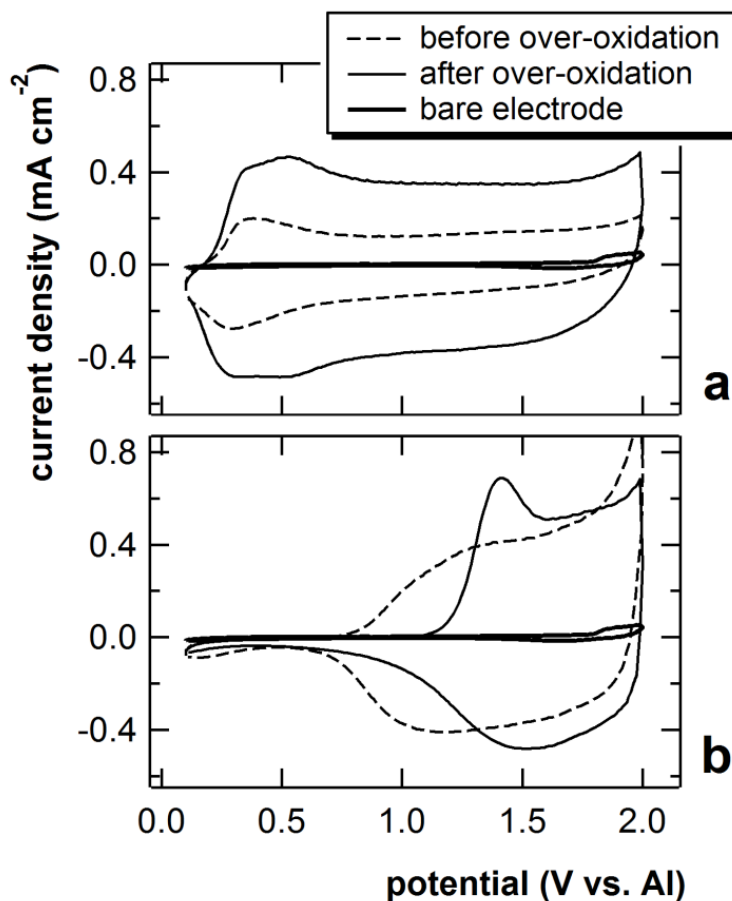
Figure 5. Cyclic voltammograms at 10 mV s^{-1} of polypyrrole (**a**) and polythiophene (**b**) films on glassy carbon substrates in three-electrode cells with 1.5:1 AlCl$_3$:EMIC at room temperature. Curves were recorded before and after oxidation to 2.6 V vs. Al ("over-oxidation"). Data for the bare glassy carbon electrode tested under the same conditions is also given in (a) and (b).

more significant extent, above 2.3 V. These anodic limits will determine the upper voltage limit of a rechargeable aluminum battery based on AlCl$_3$:EMIC.

Following ten CV cycles to an upper limit of 2.6 V, such as those shown in Figure 6, a change in the redox behavior of both polymer films at lower potentials was observed. This process is referred to here as "over-oxidation," and its effect is shown in the CV curves of Figure 5. Oxidation of the polypyrrole film to 2.6 V changed both the faradaic and non-faradaic aspects of charge transfer. Current densities were higher overall, and the redox peak-pair became broader and higher in potential, possibly splitting into two peaks. In the case of the polythiophene film, over-oxidation shifted the redox peak-pair to higher potentials and sharpened the oxidation peak. These effects have not been observed previously in other studies, and their cause or causes were not identified in this study. One possible explanation is that the polymers became chlorinated upon oxidation, forming poly(3-chlorothiophene) or poly(3,4-dichlorothiophene), due to the high amount of chloroaluminate species in the electrolyte. As was previously demonstrated, substitu-
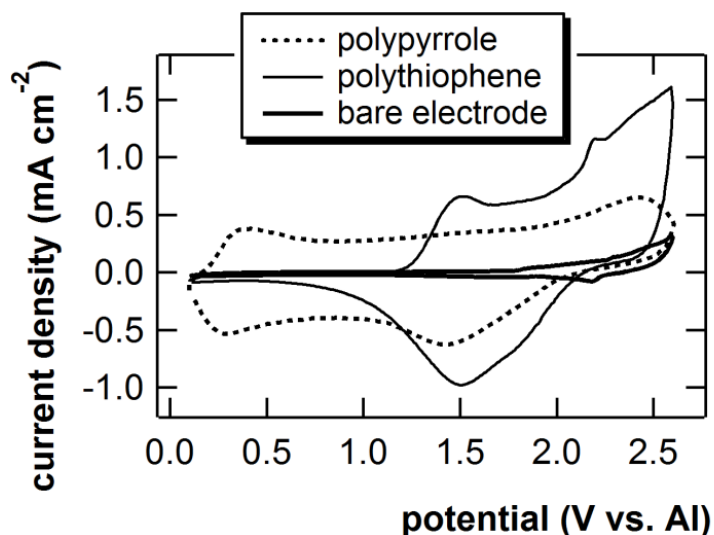
Figure 6. Cyclic voltammograms at 10 mV s^{-1} of polypyrrole and poly-thiophene films on glassy carbon substrates and of the bare glassy carbon electrode in three-electrode cells with 1.5:1 AlCl$_3$:EMIC at room temperature.

tion of halogens on the β positions of thiophene rings in polythiophene can result in an upward shift in redox potential by as much as 0.4 V.[43] Such a change in polymer chemistry could also change the morphology and surface characteristics of the bulk polymer film, which would have an effect on non-faradaic electrochemical behavior.

Following cyclic voltammetry experiments, galvanostatic cycling was performed on the electropolymerized, over-oxidized films in 1.5:1 AlCl$_3$:EMIC vs. aluminum counter and reference electrodes as an initial evaluation of their suitability for rechargeable batteries. Potential profiles are shown in Figure 7 for cycling at 10 μA cm^{-2} with various voltage limits above 0.6 V vs. Al. Considering the capacities per unit area achieved in both polymers, the current density corresponds to a cycling rate of "1C" (one charge or discharge per hour). The potential profiles of polypyrrole films were more sloping throughout the voltage range than those of polythiophene due to the non-faradaic nature of the charge transfer in these potential ranges. For polypyrrole, there was not a strong dependence of capacity on voltage limits. By contrast, polythiophene has a sloping voltage profile only above ~1 V; at lower potentials, it exhibited negligible capacity, as in the CV results. Thus, the capacities achieved in polythiophene films were more dependent on voltage limits, and significantly higher capacities were achieved with the voltage limits at higher values. For both polymer films, charging up to 1.9 V resulted in non-negligible amount of irreversible capacity. Also shown in Figure 7 is the effect of over-oxidation of the polymer films on the galvanostatic cycling profile. Over-oxidation did not have a strong effect on the voltage profile of polypyrrole at this cycling rate and over this voltage range, but it did produce a slight shift upward in voltage for polythiophene, which is in agreement with the CV observation.
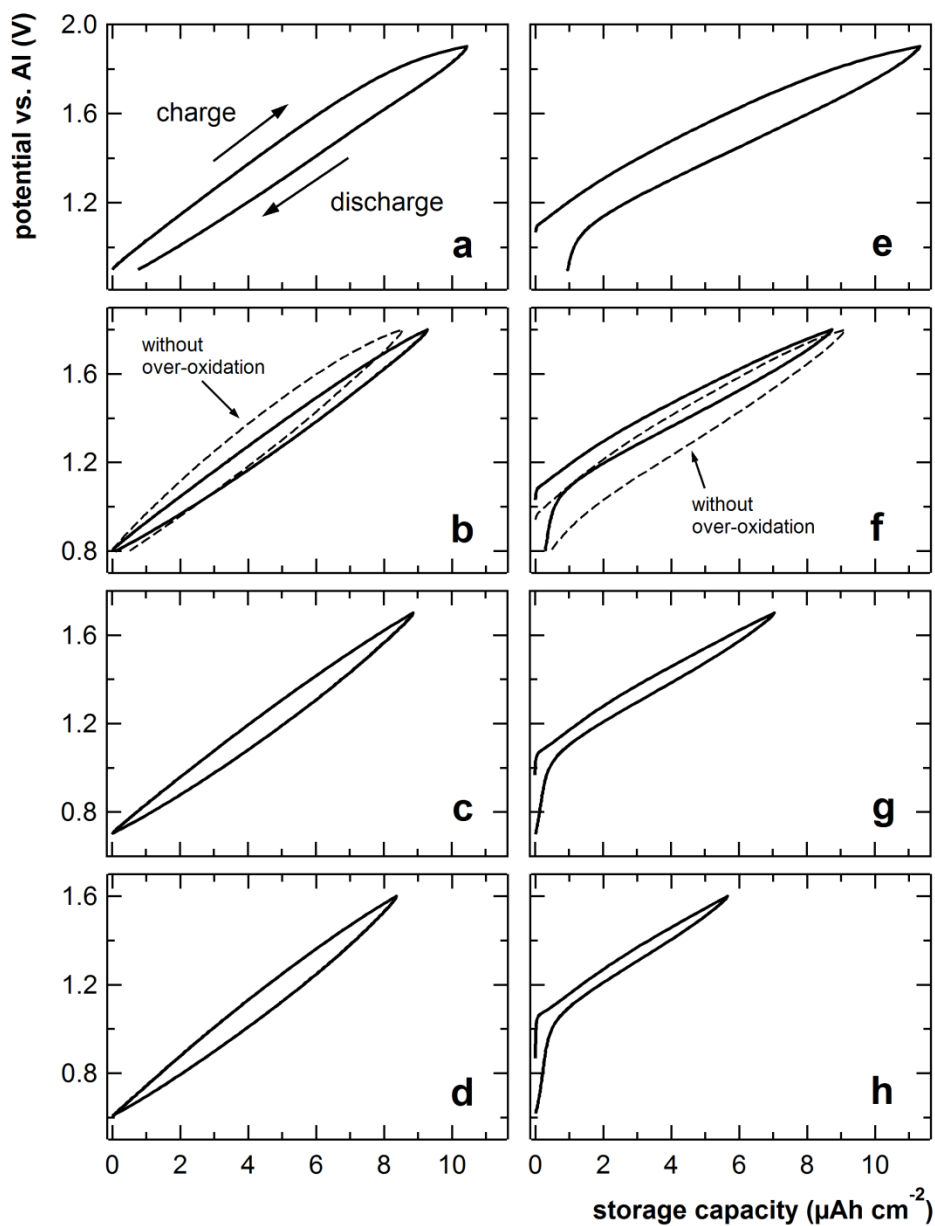
Figure 7. Potential profiles for galvanostatic cycling at room temperature of polypyrrole (**a** – **d**) and polythiophene (**e** – **h**) films on glassy carbon. Three-electrode cells with 1.5:1 AlCl$_3$:EMIC as electrolyte and aluminum as counter and quasi-reference electrodes were used. The fifth cycle is shown in each case. Cycling rate for charge and discharge was 10 μA cm^{-2}. Voltage ranges were 0.9 – 1.9 V (**a** and **e**), 0.8 – 1.8 V (**b** and **f**), 0.7 – 1.7 V (**c** and **g**), and 0.6 – 1.6 V (**d** and **h**).

Cycling stability of the conducting polymers in aluminum cells was evaluated by cycling polypyrrole and polythiophene film-electrodes fifty times with three different sets of voltage limits. The capacity per unit area and coulombic efficiency (discharge capacity divided by charge capacity) of polypyrrole electrodes as a function of cycle number are shown in Figure 8. Cycling

25

was relatively stable over 50 cycles, especially within the voltage limits 0.8 – 1.8 V. There was a slight dependence of capacity on voltage range, with higher capacities achieved at higher voltages. The lower coulombic efficiencies at higher voltages were most likely due to irreversible chlorine evolution, as discussed above.[42] Nevertheless, the average coulombic efficiencies for cycling over 0.8 – 1.8 V were close to 99%. The gravimetric capacities, given on the right axis of Figure 8a, were estimated by multiplying the area-specific capacity by the EQCM-measured mass loadings from Table 1. This gravimetric capacity is specific to the mass of doped polymer. Theoretically, polypyrrole doped with one $AlCl_4^-$ per four monomers (the composition determined above) would have a gravimetric capacity of 61.3 mAh g^{-1}, approximately two times that of the observed values. Given the significant amount of electrochemical activity observed over a broad voltage range in the CV, especially at lower voltages, the theoretical capacity could likely be achieved by using a wider voltage range for polypyrrole cycling. This was not attempted in the present study because broader potential ranges are less useful for battery applications.

Figure 8. Discharge capacity (**a**) and coulombic efficiency (**b**) for galvanostatic cycling of over-oxidized polypyrrole film electrodes. Voltage limits are given in the legend. Other conditions as in Figure 7. Markers and error bars are the average and standard deviation, respectively, of four identically prepared samples. Gravimetric capacity on the right axis was estimated using the mass loadings measured by EQCM (Table 1).
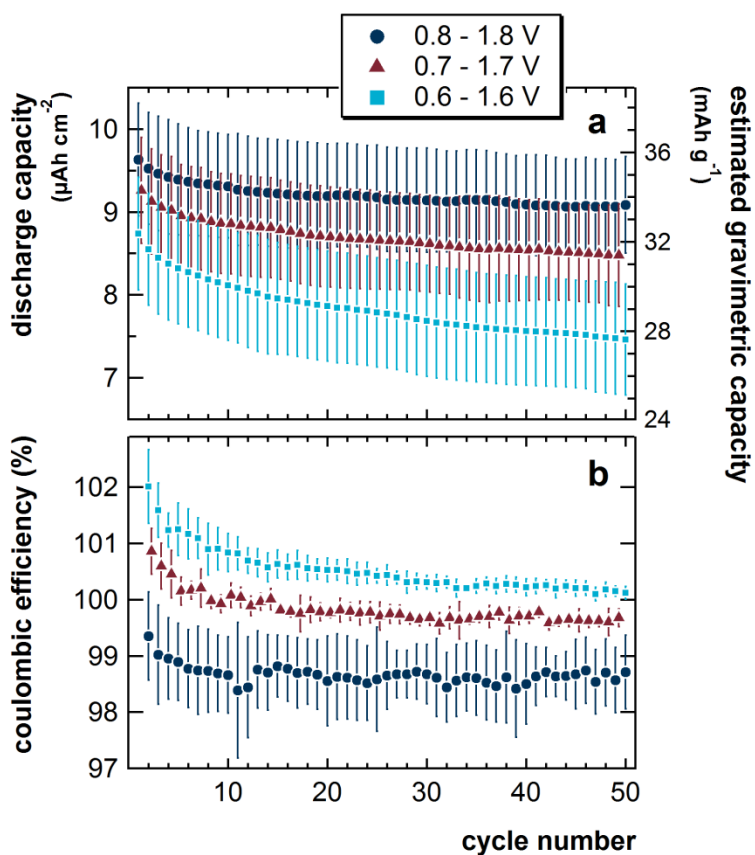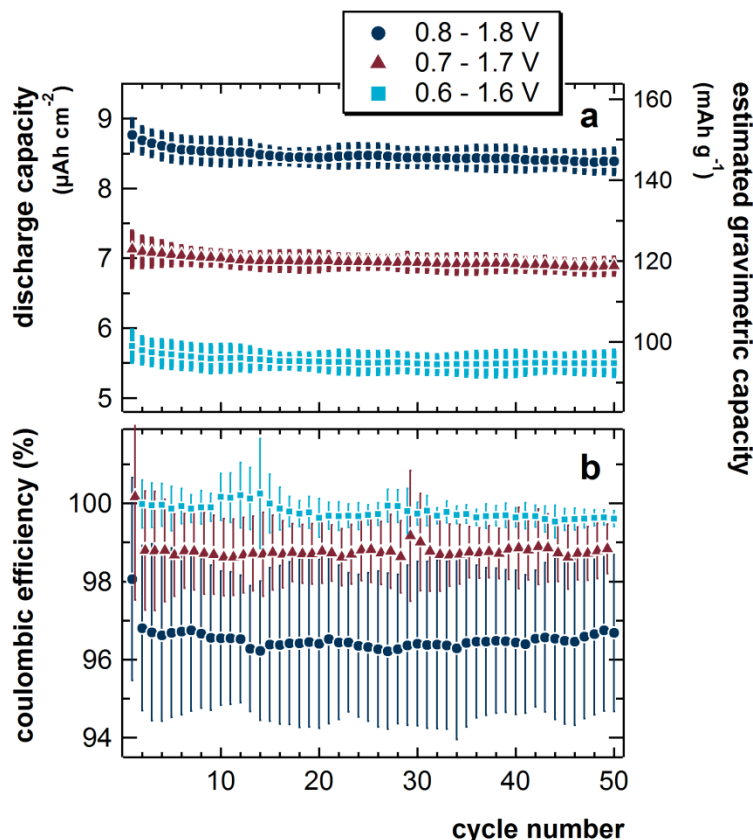
Figure 9. Discharge capacity (**a**) and coulombic efficiency (**b**) for galvanostatic cycling of over-oxidized polythiophene film electrodes. Voltage limits are given in the legend. Other conditions as in Figures 7 and 8.

The capacity per unit area and coulombic efficiency of polythiophene electrodes as a function of cycle number are shown in Figure 9. Cycling was very stable over 50 cycles for each set of voltage limits. There was a strong dependence of capacity on voltage range, with capacities for the $0.8 - 1.8$ V range being 50% higher than those for the $0.6 - 1.6$ V range. As with polypyrrole, higher capacities corresponded to lower coulombic efficiencies. Chlorine evolution seemed to be slightly more significant in polythiophene than in polypyrrole because the average coulombic efficiencies were slightly lower. Nevertheless, the coulombic efficiencies ranged from 96% to 100%, indicating excellent reversibility. The gravimetric capacities, given on the right axis of Figure 9a, were significantly higher than those of polypyrrole. Theoretically, polythiophene doped with one $AlCl_4^-$ per four monomers would have a gravimetric capacity of 53.0 mAh g^{-1}. The observed values are much higher than this. One possible or partial explanation for this is that polythiophene achieves a higher extent of doping than polypyrrole in this electrolyte. However, doping levels above 33% have rarely been observed in polythiophene.[21] A more likely explanation is that the polythiophene was polymerized in an undoped state. The theoretical specific capacity for undoped polythiophene is 79.6 mAh g^{-1} or 106 mAh g^{-1} for a transfer of one electron per four or three monomers, respectively. This explanation is likely because the open-circuit potentials (OCP) of polythiophene electrodes in 1.5:1 AlCl$_3$:EMIC immediately after polymerization ranged from 0.8 V to 1.1 V, which are lower values than the redox potential ob-

served in CV. Thus, the polymer after electrochemical synthesis was probably in its reduced, undoped state. The corresponding theoretical capacity values are closer to the observed values. A third possible explanation for the discrepancy is that the adhesion of electropolymerized polythiophene on QCM-platinum electrodes was worse than on glassy carbon electrodes. If this is the case, the amount of polythiophene deposited on glassy carbon would be higher than expected from the QCM measurements. Thus, the gravimetric capacity values in Figure 9 would be artificially high due to an underestimate of the polythiophene mass on the electrode.

Polythiophene film electrodes were cycled at different rates in three-electrode cells to evaluate the rate capability of the electrode reaction. The cycling behavior is shown in Figure 10, with the approximate effective "C-rates" (number of charges or discharges per hour) for each current density. The electrodes were subjected to rates of 1, 10, and 50 μA cm^{-2} over the voltage range 0.6 – 1.6 V. In general, higher current density corresponded to lower capacity and higher coulombic efficiency. However, a 50-fold increase in current density reduced the capacity by only ~20% and brought the coulombic efficiency up to 100%. This shows that the anion-insertion cycling mechanism in these conducting polymer electrodes is able to accommodate high reaction rates and thus may lead to batteries with high power output.
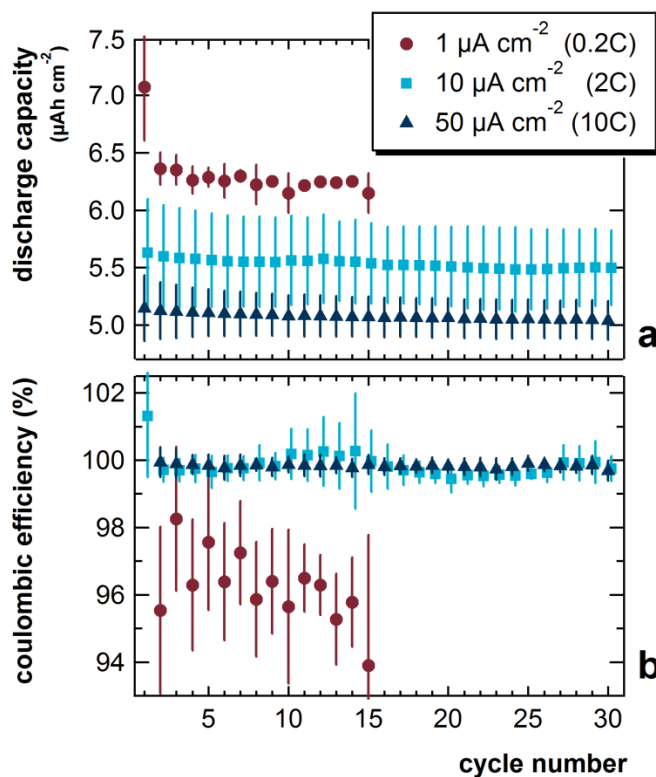
Figure 10. Discharge capacity (**a**) and coulombic efficiency (**b**) for galvanostatic cycling at room temperature of over-oxidized polythiophene film electrodes at various current densities (indicated in legend with approximate C-rate). Three-electrode cells with 1.5:1 AlCl$_3$:EMIC as electrolyte and aluminum as counter and quasi-reference electrodes were used. Voltage limits for cycling were 0.6 – 1.6 V. Markers and error bars are the average and standard deviation, respectively, of three identically prepared samples.

As a test of long-term cycling, one polythiophene film on glassy carbon was cycled four hundred times at 10 µA cm^{-2} over the voltage range 0.6 – 1.6 V. At the 10th cycle, the electrode achieved 5.66 µAh cm^{-2} discharge capacity and 100.4% coulombic efficiency; at the 400th cycle, the electrode achieved 5.64 µAh cm^{-2} discharge capacity and 99.6% coulombic efficiency. The negligible decrease in capacity and consistently high coulombic efficiency indicate excellent long-term stability and performance of the conducting polymer in CIL electrolyte.

3.5. Cycling of Sealed Sandwich-Type Cells

Composite electrodes containing commercially produced polypyrrole or polythiophene in powder form, organic polymer binder, and conductive additive (carbon black) were fabricated as a step toward prototyping of the proposed aluminum batteries. The composite electrodes are referred to as tapes (instead of coatings) because they are freestanding and not deposited on a substrate. As opposed to the flooded cells with thin-film conducting polymer electrodes tested in the glove box as described above, the electrode tapes were tested in sealed Swagelok®-type cells outside the glove box. Swagelok®-type cells are two-electrode cells with the aluminum anode, electrolyte/separator, and cathode sandwiched with a spring between current collector rods. As shown previously, the CIL electrolytes are electrochemically reactive with stainless steel electrodes, which can lead to false capacity measurements.[19] Thus the current collector on the cathode side in the present study was made of glassy carbon. The current collector on the anode side was composed of a copper rod, copper-plated spring, and copper disc. Cells with no electrode tape on the cathode side (only the glassy carbon rod) exhibited negligible capacity upon cycling, which confirmed that 1.5:1 AlCl$_3$:EMIC electrolyte was not electrochemically reactive with the cell components.

Immediately following cell assembly and prior to charge-discharge cycling, the open-circuit potentials of cells containing polypyrrole and polythiophene cathodes were 1.6 V and 1.2 V, respectively. The sealed cells were initially cycled five times at high galvanostatic rates (160 – 200 mA g^{-1} specific to the mass of active cathode material) over a broad voltage range (0.1 – 2.6 V). These "conditioning cycles" were executed in an attempt to recreate the over-oxidation effect described above and to replace any native dopants with the chloroaluminate dopants. The dopant identities and quantities of the as-received polypyrrole and polythiophene powders were unknown as of this writing of this report.

Following the conditioning cycles, cells with polypyrrole and polythiophene cathodes were cycled galvanostatically at rates of 20 mA g^{-1} and 16 mA g^{-1}, respectively. Each of these specific current values corresponds to the theoretical cycling rate of 0.2C if the polymer is assumed to be undoped with the capacity for one electron equivalent transferred per four monomers (99.9 mAh g^{-1} for polypyrrole and 79.6 mAh g^{-1} for polythiophene). Potential profiles for the fifth and one-hundredth cycle at these rates with voltage limits of 0.8 V and 2.0 V are shown in Figure 11. Polypyrrole reached about half its theoretical capacity, which is evidence that the as-received powder is in a doped or partially-doped state. The shape of the potential curve did not change significantly with cycling despite the loss of capacity. The subtle potential plateau around 1.3 V suggests a faradaic process, which was unexpected given the lower redox potential observed in CV experiments. The cause of this discrepancy is unknown, but it may be due to a chemical or structural difference between electrochemically and chemically synthesized forms of polypyrrole. By contrast, the polythiophene potential curve did not exhibit any obvious plateau.
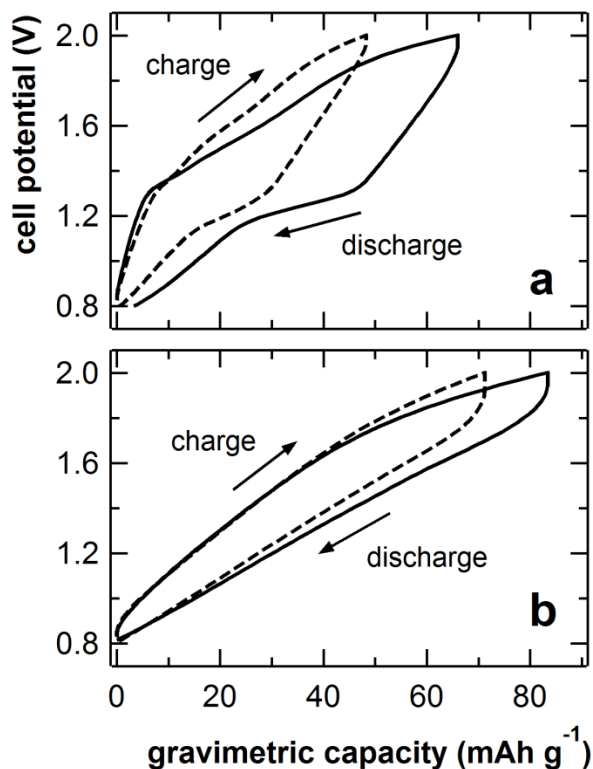
Figure 11. Potential profiles for galvanostatic cycling at 30°C of sealed Swagelok-type cells containing polypyrrole (**a**) and polythiophene (**b**) composite cathodes with 1.5:1 $AlCl_3$:EMIC as electrolyte and aluminum metal anode. Specific currents were 20 mA g^{-1} (**a**) and 16 mA g^{-1} (**b**) relative to the mass of active material at the cathode. Gravimetric capacity values are also relative to the mass of active material at the cathode. Voltage limits for cycling were 0.8–2.0 V. The 5th cycle (solid line) and 100th cycle (dashed line) are shown in each case.

However, it was electrochemically active in the same potential range as that of the CV study. The polythiophene cells reached theoretical capacity. ~80 mAh g^{-1} relative to the mass of un-doped polymer. Thus, it is highly likely that the commercial polythiophene powder is in an un-doped form; otherwise, it would be difficult to reach such high gravimetric capacity.

The observations that the polypyrrole powder is initially in a doped form and the polythiophene powder is in an undoped form are further supported by the initial OCP values given above. The polypyrrole cell exhibited a relatively high OCP, above the redox potential of polypyrrole. The polythiophene cell exhibited a relatively low potential, below the redox potential of polythiophene observed in CVs. Further proof of this is the fact that the undoped form of polypyrrole is unstable in air[36] (the environment in which the electrode tapes were fabricated), while polythiophene is air-stable whether in a doped or undoped form.[44]

The achievement of theoretical capacity for undoped polythiophene confirms that the amount of charge stored is approximately one electron transferred per four thiophene monomers.

Thus, the identity of the arbitrary cathode host X in Equation 4 is four molecules of thiophene, and the overall gravimetric capacity is 30.2 mAh g^{-1} relative to the combined mass of all active cell components (aluminum metal anode, AlCl$_3$:EMIC electrolyte, and polythiophene cathode). This value can be multiplied by the average cell potential (1.47 V as measured from the 5th-cycle data in Figure 11b) to obtain a specific energy of 44.4 Wh kg^{-1}. For polypyrrole, this calculation is more difficult because the doping level cannot be determined from the data in Figure 11a. If the assumption of four monomers per electron transferred holds for polypyrrole in powder form, as it did for the electrodeposited samples, then a specific energy of 46.4 Wh kg^{-1} is calculated (using the average cell potential from Figure 11a, 1.42 V).

Continued cycling behavior for the first 100 cycles of polypyrrole and polythiophene cells at 20 mA g^{-1} and 16 mA g^{-1} are shown in Figure 12. Data for several ranges of voltage limits were tested, and the expected trend of higher capacity for higher voltages was observed for the sealed cells, as it was for the cells with electrodeposited polymer. Capacities measured for the sealed polypyrrole cells were roughly in agreement with those of the electropolymerized films above. Capacities measured for the sealed polythiophene cells were less than half of those of the electropolymerized films. This may be due to inaccuracies with the QCM measurements, as described above, or to chemical or structural differences between electropolymerized films and powders. Coulombic efficiencies for the sealed polypyrrole and polythiophene cells of Figure 12 were greater than 91% and 96%, respectively, but a clear relationship to voltage limits was not observed. Also shown in Figure 12b is the cycling behavior of a cell with MCMB composite tape as the cathode, cycled with the same voltage limits as the polymer cells. MCMB is a carbonaceous material commonly used for lithium-ion battery electrodes. It was used here as a control, to test whether the observed capacities were simply the result of a surface reaction that would occur on any conductive material or on the conductive additive (carbon black). As shown, the capacities of the MCMB cell were significantly lower than all of those with the conducting polymer cells. Thus, the observed capacities are unique to the conducting polymers and most likely arise from the proposed anion-doping reaction.

For a proof-of-concept demonstration, the results in Figure 12 show excellent cycling stability. Between the 20th and 100th cycles, the polypyrrole cells exhibited 14–26% loss in capacity, and the polythiophene cells exhibited only 13% loss. Upon disassembly of all the cells, the electrolyte and separator appeared to be contaminated with dark-colored material. Thus, the most likely cause of capacity decay was loss of the active material to the electrolyte solution. Although the electropolymerized films were not prone to dissolution in the electrolyte, as evidenced by their cycling behavior and appearance, it is very likely that the polymer binder in the electrode tapes does not completely confine the conducting polymers to the electrode. Indeed, some disintegration of the electrode tapes was visually observed when they were placed in a vial full of AlCl$_3$:EMIC electrolyte. The binder itself may dissolve or degrade in the electrolyte. This particular binder material is common to lithium-ion electrodes, and it is quite possible that the chemistry used in this study requires a different type of binder. The binder in any such composite electrode must serve the dual purpose of confining the other electrode materials whilst allowing ion transport (often via solvent swelling) to the active material. It is unclear whether the electrolyte-binder combination in this study allows swelling and ion transport without completely dissolving and releasing the active materials. Thus, higher capacities and better cycling could be achieved with an optimal binder material. Nevertheless, the loss of active electrode material to the electrolyte in the cells of the present study does not appear to short the cells or to greatly alter their voltages, as shown in the comparisons between the 5th and 100th cycles in Figure 11.
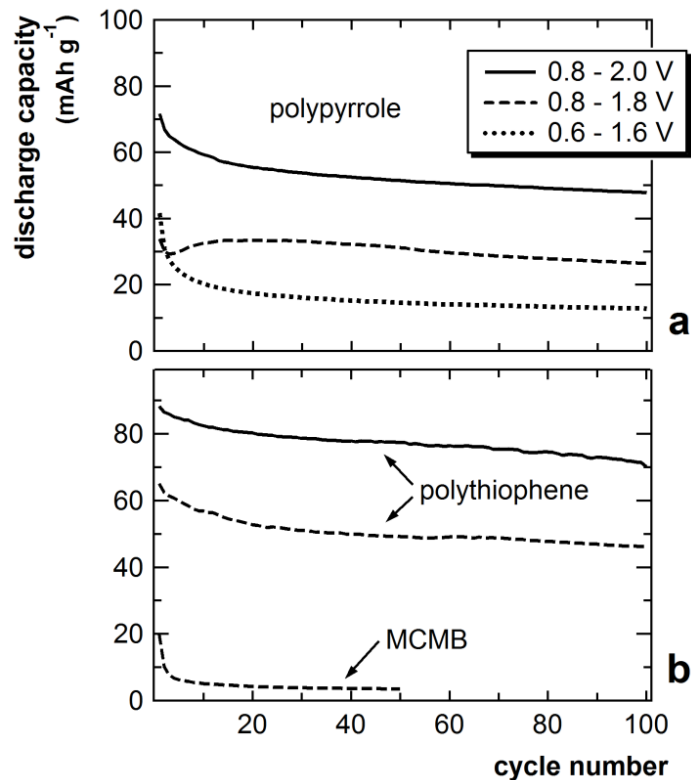
Figure 12. Discharge capacities for galvanostatic cycling at 30°C of sealed Swagelok-type cells containing polypyrrole (**a**), polythiophene (**b**), and MCMB (**b**) composite cathodes. Specific currents were 20 mA g^{-1} (polypyrrole and MCMB) and 16 mA g^{-1} (polythiophene) relative to the mass of active material at the cathode. Discharge capacity values are also relative to the mass of active material at the cathode. Voltage limits for cycling are indicated in legend.

4. CONCLUSIONS

Presented here are a proof-of-concept and quantitative evaluation of conducting polymers (polypyrrole and polythiophene) as active materials for the positive electrode in rechargeable aluminum batteries operating at room temperature. This battery chemistry is based on acidic chloroaluminate ionic liquids, with which aluminum metal can be reversibly stripped and plated at the negative electrode. Previous demonstrations showed that these materials could potentially be useful in aluminum-based batteries. However, they lacked understanding of the fundamental cycling mechanisms and quantitative cell characterization with battery-relevant conditions and metrics.

The electrochemical synthesis and characterization of conducting polymer films on glassy carbon electrodes with CIL electrolyte was performed to investigate cycling mechanisms and fundamental electrochemical performance of the materials. FTIR spectroscopy, mass measurements with a laboratory balance, and elemental analysis were used to prove that polypyrrole films synthesized in this way were doped with chloroaluminate anions from the electrolyte solution. The doping level was measured as approximately four monomer units per anion dopant molecule. Cyclic voltammetry showed faradaic and non-faradaic electrochemical activity in both polypyrrole and polythiophene, with the electrochemical activity of polythiophene concentrated at higher potentials (above 1 V vs. Al metal). Galvanostatic cycling of both types of polymer films was highly stable, showing negligible losses in capacity after 50–400 cycles. The high coulombic efficiencies approaching 100% showed that anion-doping of the polymers in CIL electrolytes is highly reversible and appropriate for a rechargeable battery. The cycling behavior of polythiophene exhibited a strong dependence on voltage limits, with higher voltages produces higher capacity and lower coulombic efficiency. Electrochemical quartz-crystal microbalance was used during electrochemical polymerization to estimate the amount of deposited mass on the electrode, and these values were used to estimate gravimetric capacities. The resultant estimates of 30–100 mAh g^{-1} (specific to polymer mass) were on par with theoretically-predicted values. The polythiophene electrodes also exhibited excellent rate capabilities, with minor decreases in cycling capacity when the current density was increased fifty-fold.

Prototypes of the aluminum battery cells were assembled by preparing composite electrodes containing polypyrrole or polythiophene powder with organic polymer binder and conductive carbon additive. These electrodes were combined with CIL-soaked separator and aluminum metal anode in a sandwich configuration in sealed Swagelok®-type cells. Although the galvanostatic cycling of these cells was not as stable as that of the electropolymerized films, they retained a significant amount of capacity with high coulombic efficiency after 100 cycles. Losses in capacity were attributed to the loss of active material to the electrolyte, but this did not cause cell shorting or changes in the cycling potential. This problem could be addressed by developing better binders for the material system here. The capacities measured in sealed prototype cells were 30–100 mAh g^{-1}, in agreement with those measured for electropolymerized films. These values were used with observed cell voltages to estimate the gravimetric energy density relative to the active cell components. The energy density of the polythiophene-CIL-aluminum cell chemistry was estimated as 44 Wh kg^{-1}, and that of the polypyrrole-CIL-aluminum cell was 46 Wh kg^{-1}. These energy densities are competitive for grid-scale energy storage; they are on par with those of flow battery[2, 45, 46] and lead-acid[2, 47] systems. As battery components based vanadium, lead, lithium, and cobalt continue to become more expensive and limited in supply, the

type of aluminum batteries presented here may have a competitive edge based on their potential cost and safety advantages.

Despite the promising results presented here, there are limitations of the proposed battery chemistry. For both polypyrrole and polythiophene cells, significantly sloping voltage profiles for charge and discharge were observed. This will limit the amount of practical voltage that can be obtained from the battery for a full discharge. Furthermore, attempts to operate at voltages above 1.9 V reduce the coulombic (round-trip) efficiency of the cells to below 90%. The irreversible reactions at higher voltages will consume the ionic liquid electrolyte and lead to capacity losses. This highlights another limitation of the battery chemistry, which is the active participation of the chloroaluminate electrolyte in the electrode reaction. In contrast to rocking-chair batteries, cell capacity in the anion-insertion chemistry presented here is dependent on the amount of electrolyte. The amount of CIL must scale with the size of the anion-insertion electrodes, but the minimum required amount of CIL must be used to achieve the highest possible energy density (unlike the demonstrations presented here, in which an excess of electrolyte was used). In this case any losses of electrolyte through irreversible reaction or precipitation would reduce the cell's effective capacity. Nevertheless, the results presented here prove that an aluminum-based battery operating at room temperature, with a cycling aluminum-metal anode, can exhibit excellent stability and efficiency (up to hundreds of cycles) and competitive energy density. Increased understanding of the electrode reaction mechanisms may lead to more informed design of active electrode materials with increased capacity or more desirable voltage profiles. Furthermore, the modification of CIL electrolytes or the use of alternative electrolytes, which was not explored here, may allow for higher voltage limits and lead to increased energy density and efficiency.
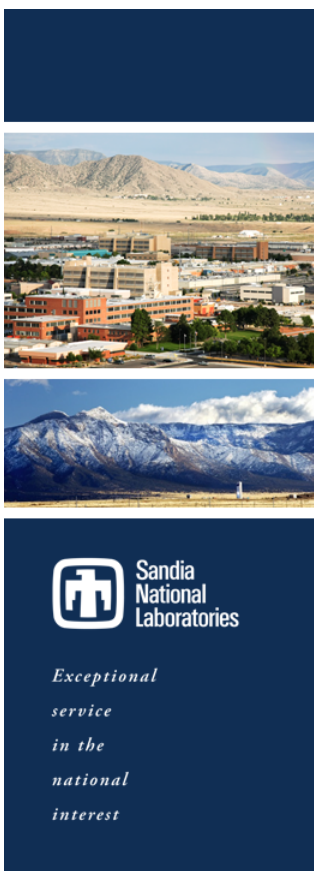
5. REFERENCES

1. M. M. Thackeray, C. Wolverton and E. D. Isaacs, *Energy Environ Sci*, 2012, **5**, 7854-7863.

2. Z. Yang, J. Zhang, M. C. W. Kintner-Meyer, X. Lu, D. Choi, J. P. Lemmon and J. Liu, *Chem Rev*, 2011, **111**, 3577-3613.

3. C. Wadia, P. Albertus and V. Srinivasan, *J Power Sources*, 2011, **196**, 1593-1598.

4. *Mineral Commodity Summaries*, U. S. Geological Survey, 2013.

5. Q. F. Li and N. J. Bjerrum, *J Power Sources*, 2002, **110**, 1-10.

6. J. J. Auborn and Y. L. Barberio, *J Electrochem Soc*, 1985, **132**, 598-601.

7. J. S. Wilkes, J. A. Levisky, R. A. Wilson and C. L. Hussey, *Inorg Chem*, 1982, **21**, 1263-1264.

8. T. Jiang, M. J. C. Brym, G. Dube, A. Lasia and G. M. Brisard, *Surf Coat Tech*, 2006, **201**, 1-9.

9. P. K. Lai and M. Skyllas-Kazacos, *J Electroanal Chem*, 1988, **248**, 431-440.

10. A. A. Fannin, D. A. Floreani, L. A. King, J. S. Landers, B. J. Piersma, D. J. Stech, R. L. Vaughn, J. S. Wilkes and L. Williams John, *J Phys Chem*, 1984, **88**, 2614-2621.

11. K. Xu, *Chem Rev*, 2004, **104**, 4303-4418.

12. N. Ingale, J. Gallaway, D. Steingart, S. Khatun, P. Sideris, S. Greenbaum, S. Banerjee and A. Couzis, *The Electrochemical Society Meeting Abstracts*, 2011, **MA2011-01**, 1519.

13. N. Koura, H. Tsuda and K. Ui, *Denki Kagaku*, 1996, **64**, 1195-1199.

14. P. R. Gifford and J. B. Palmisano, *J Electrochem Soc*, 1988, **135**, 650-654.

15. F. M. Donahue, S. E. Mancini and L. Simonsen, *J Appl Electrochem*, 1992, **22**, 230-234.

16. M. P. Paranthaman, G. Brown, X.-G. Sun, J. Nanda, A. Manthiram and A. Manivannan, *The Electrochemical Society Meeting Abstracts*, 2010, **MA2010-02**, 314.

17. N. Jayaprakash, S. K. Das and L. A. Archer, *Chem Comm*, 2011, **47**, 12610-12612.

18. J. V. Rani, V. Kanakaiah, T. Dadmal, M. S. Rao and S. Bhavanarushi, *J Electrochem Soc*, 2013, **160**, A1781-A1784.

19. L. D. Reed and E. Menke, *J Electrochem Soc*, 2013, **160**, A915-A917.

20. E. Levi, Y. Gofer and D. Aurbach, *Chem Mater*, 2009, **22**, 860-868.

21. P. Novak, K. Muller, K. S. V. Santhanam and O. Haas, *Chem Rev*, 1997, **97**, 207-281.

22. P. G. Pickup and R. A. Osteryoung, *J Electroanal Chem*, 1985, **195**, 271-288.

23. L. Janiszewska and R. A. Osteryoung, *J Electrochem Soc*, 1987, **134**, 2787-2794.

24. J. Tang and R. A. Osteryoung, *Synthetic Met*, 1991, **45**, 1-13.

25. L. M. Goldenberg and R. A. Osteryoung, *Synthetic Met*, 1994, **64**, 63-68.

26. K. Takeishi and N. Koura, *Denki Kagaku*, 1995, **63**, 947-951.

27. K. Ui, Y. Kuma and N. Koura, *Electrochemistry*, 2006, **74**, 536-538.

28. N. Koura and H. Ejiri, *Denki Kagaku*, 1990, **58**, 923-927.

29. N. Koura, H. Ejiri and K. Takeishi, *Denki Kagaku*, 1991, **59**, 74-75.

30. N. Koura, H. Ejiri and K. Takeishi, *J Electrochem Soc*, 1993, **140**, 602-605.

31. B. J. Tierney, W. R. Pitner, J. A. Mitchell, C. L. Hussey and G. R. Stafford, *J Electrochem Soc*, 1998, **145**, 3110-3116.

32. P. G. Pickup and R. A. Osteryoung, *J Am Chem Soc*, 1984, **106**, 2294-2299.

33. D. A. Buttry and M. D. Ward, *Chem Rev*, 1992, **92**, 1355-1379.

34. A. S. Gozdz, C. N. Schmutz, J.-M. Tarascon and P. C. Warren, ed. USPTO, Bell Communications Research, Inc., United States of America, Editon edn., 1993, vol. 5,418,091.

35. D. Orata and D. A. Buttry, *J Am Chem Soc*, 1987, **109**, 3574-3581.

36. G. B. Street, in *Handbook of Conducting Polymers: Volume 1*, ed. T. A. Skotheim, Marcel Dekker, Inc., New York, 1986, vol. 1, pp. 265-291.

37. B. Tian and G. Zerbi, *J Chem Phys*, 1990, **92**, 3886-3891.

38. A. F. Diaz and J. Bargon, in *Handbook of Conducting Polymers: Volume 1*, ed. T. A. Skotheim, Marcel Dekker, Inc., New York, 1986, vol. 1, pp. 81-115.

39. C. L. Hussey, T. B. Scheffler, J. S. Wilkes and A. A. Fannin, *J Electrochem Soc*, 1986, **133**, 1389-1391.

40. K. S. Mohandas, N. Sanil, M. Noel and P. Rodriguez, *Carbon*, 2003, **41**, 927-932.

41. M. Noel and R. Santhanam, *J Power Sources*, 1998, **72**, 53-65.

42. Z. J. Karpinski and R. A. Osteryoung, *Inorg Chem*, 1984, **23**, 1491-1494.

43. R. J. Waltman, J. Bargon and A. F. Diaz, *J Phys Chem*, 1983, **87**, 1459-1463.

44. G. Tourillon, in *Handbook of Conducting Polymers: Volume 1*, ed. T. A. Skotheim, Marcel Dekker, Inc., New York, 1986, vol. 1, pp. 293-350.

45. M. Skyllas-Kazacos, M. H. Chakrabarti, S. A. Hajimolana, F. S. Mjalli and M. Saleem, *J Electrochem Soc*, 2011, **158**, R55-R79.

46. M. Skyllas-Kazacos, G. Kazacos, G. Poon and H. Verseema, *Int J Energy Res*, 2010, **34**, 182-189.

47. T. B. Reddy and D. Linden, *Linden's handbook of batteries*, 4th edn., McGraw-Hill, New York, 2011.

APPENDIX A:
PRESENTATION SLIDES FROM
THE ELECTROCHEMICAL SOCIETY MEETING (MAY 2013)

The slides below were from a presentation given by the author at the semi-annual conference and meeting of The Electrochemical Society. The slides contain additional information and data not discussed above, including scanning electron microscope (SEM) images and a study of the effect of using halogen-substituted monomers to create halogen-substituted conducting polymers for use in the electrodes of CIL-based aluminum batteries.

# Motivation for Aluminum Batteries

Aluminum is abundant and widely produced compared to other energy-storage metals.

elemental abundance in Earth's crust (kg kg^{-1})
CRC Handbook of Chemistry and Physics

worldwide metal production excluding U.S. (tonnes)
U.S. Geological Survey
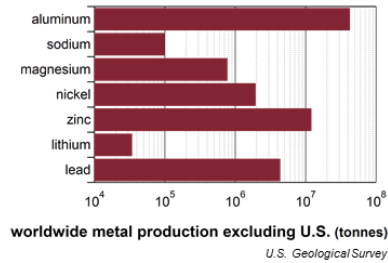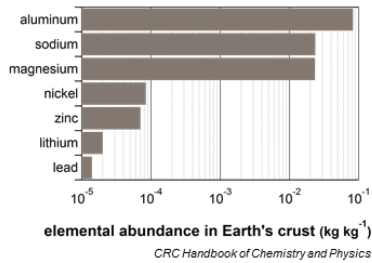
Aluminum metal's charge-storage capacity is competitive on gravimetric *and* volumetric scales.

gravimetric charge-storage capacity (Ah g^{-1})

volumetric charge-storage capacity (Ah cm^{-3})
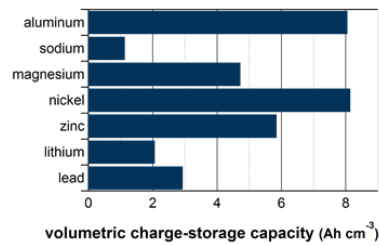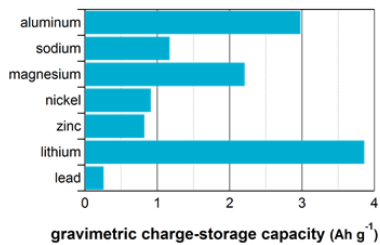
2

History of Aluminum Batteries

Aqueous Systems

- All primary cells
    - Al metal can not be electrodeposited
    - Al corrodes in alkaline electrolytes
- Aluminum-MnO$_2$
    - AlCl$_3$ or Al(OH)$_3$ electrolytes
    - Analogous to alkaline primary (Zn) cells
    - Surface oxide → decreased potential
- Aluminum-sulfur
    - K$_2$S-KOH electrolyte
    - 650 Wh kg^{-1} theoretical
- Aluminum-air
    - Alkaline or saline electrolyte
    - Reduction of oxygen at cathode
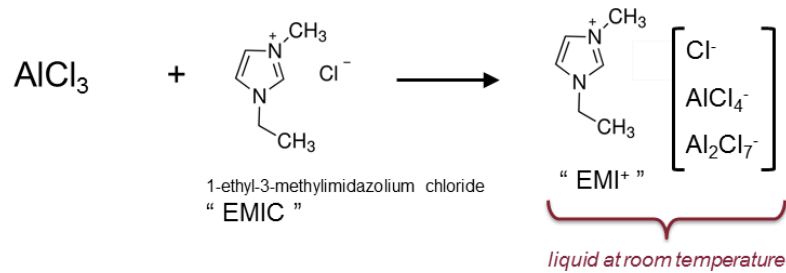   - 2800 Wh kg^{-1} theoretical
    - Mechanical recharging is possible

Q. F. Li and N. J. Bjerrum, *J Power Sources*, **110**, 1-10 (2002)

Non-Aqueous Systems

- Molten-salt electrolytes
    - NaCl-AlCl$_3$ or NaCl-KCl-AlCl$_3$
    - 100ºC – 300ºC operation
    - Chlorine cathodes
        - Recapture of chlorine at electrode is main challenge
    - Metal-chloride or metal-sulfide cathodes
        - Solubility of these species in electrolyte is main challenge
- Chloroaluminate room-temperature ionic liquids
    - Mixtures of imidazolium chlorides and aluminum chlorides
        - Efficient deposition and stripping of Al
    - Safety: low temperature & non-flammable
    - Metal-chloride or metal-sulfide cathodes
        - Solubility causes self-discharge
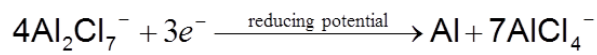   - Cathodes that are hosts for chlorine or chloroaluminate anions

3

Chloroaluminate Ionic Liquids

1-ethyl-3-methylimidazolium chloride
" EMIC "

" EMI$^+$ "

liquid at room temperature

Electrodeposition of aluminum metal is possible only when $Al_2Cl_7^-$ ions are present.

$$4Al_2Cl_7^- + 3e^- \xrightarrow{\text{reducing potential}} Al + 7AlCl_4^-$$

(Stripping of aluminum metal occurs in any stable EMIC/AlCl$_3$ mixture.)

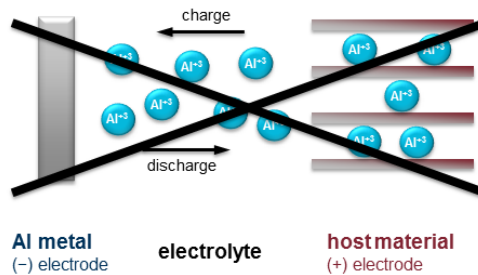This is the negative electrode in a rechargeable aluminum-metal battery.

Proposed Electrode Reactions

What about the positive electrode in a rechargeable aluminum-metal battery?

Shuttle Mechanism

- Basis for "rocking chair" batteries
- Analogous to lithium-metal batteries
- Solvated Al^{+3} ions are not present in the chloroaluminate ionic liquids
- Intercalation of trivalent species in any host is difficult and has not been successfully demonstrated with this electrolyte system
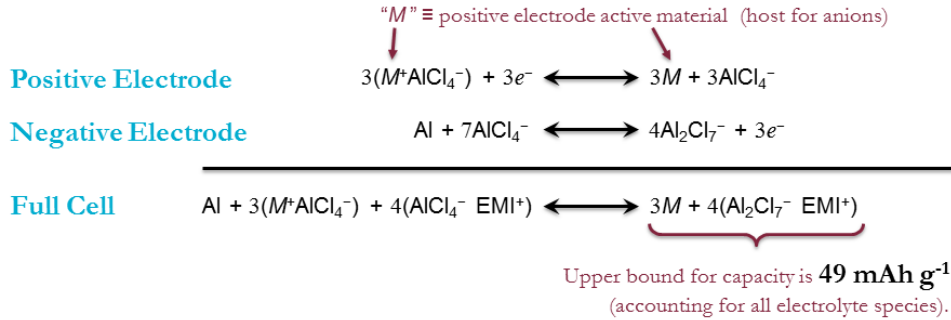
Anion-Insertion Mechanism

- AKA "dual-ion" system
- Chloroaluminate anions are inserted into positive electrode host during charge
- Amount of electrolyte must scale with the size of the positive electrode
- Demonstrated previously in
  - graphite (via intercalation of anions)
 - **conductive polymers** (via doping)

Al metal
(−) electrode

electrolyte

host material
(+) electrode

39

Proposed Electrode Reactions

Sandia National Laboratories

"M" ≡ positive electrode active material (host for anions)

Positive Electrode $3(M^+AlCl_4^-) + 3e^- \longleftrightarrow 3M + 3AlCl_4^-$

Negative Electrode $Al + 7AlCl_4^- \longleftrightarrow 4Al_2Cl_7^- + 3e^-$

Full Cell $Al + 3(M^+AlCl_4^-) + 4(AlCl_4^-\ EMI^+) \longleftrightarrow 3M + 4(Al_2Cl_7^-\ EMI^+)$
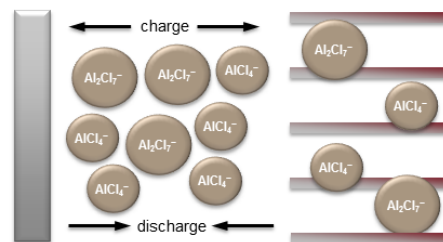
Upper bound for capacity is **49 mAh g^{-1}**
(accounting for all electrolyte species).

Anion-Insertion Mechanism

- AKA "dual-ion" system
- Chloroaluminate anions are inserted into positive electrode host during charge
- Amount of electrolyte must scale with the size of the positive electrode
- Demonstrated previously in
  - graphite (via intercalation of anions)
  - **conductive polymers** (via doping)

6
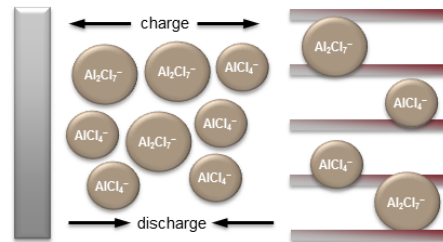
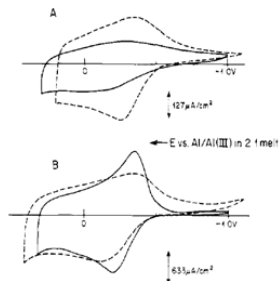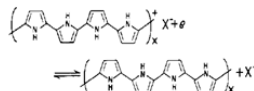# Anion-Insertion Electrodes in Chloroaluminate Ionic Liquids

Sandia National Laboratories

Polypyrrole

Figure 4. Cyclic voltammetry of Pt/polypyrrole electrodes in 0.8:1 AlCl$_3$:BuPyCl melt (—) and in 0.1 M Et$_4$NClO$_4$/CH$_3$CN (---). (A) 0.06-μm PP film prepared in CH$_3$CN, (B) 0.20-μm film prepared in neutral melt. Scan speed = 100 mV/s.

P. G. Pickup and R. A. Osteryoung,
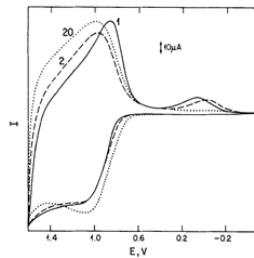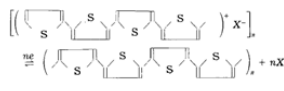*JACS*, **106**, 2294-2299 (1984)

Polythiophene

Fig. 3. Cyclic voltammetric curves for 2 × 10⁻⁴C film of polythiophene in 1:1 melt; v = 50 mV s⁻¹. Electropolymerization of thiophene was carried out in 0.1M solution of monomer in 1:1 melt at +1.7V. The number on the curve refers to the number of the scan (tungsten electrode, A = 0.12 cm²).

L. Janiszewska and R. A. Osteryoung,
J Electrochem Soc, **134**, 2787-2794 (1987)

Polyaniline
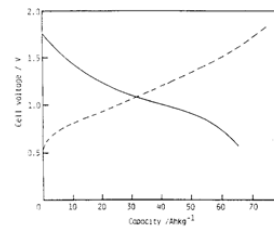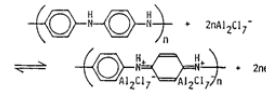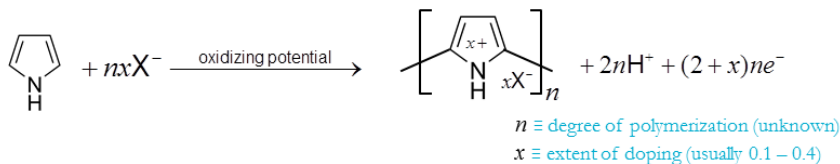

Fig.2 Chrge and discharge curves for the powder electrode of Al/PAn secondary cell.
C.D.: 2.0 mAcm⁻²
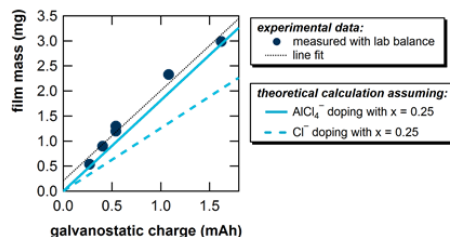----- : charge, —— : dischrge

N. Koura and H. Ejiri,
Denki Kagaku, **58**, 923-927 (1990)

7

40

Sample Prep: Electropolymerization

- Pyrrole and other conjugated monomers can be polymerized easily via electrochemical oxidation

$$\text{pyrrole} + nx\text{X}^- \xrightarrow{\text{oxidizing potential}} \left[\text{polypyrrole}^{x+} \cdot x\text{X}^- \right]_n + 2n\text{H}^+ + (2+x)ne^-$$

$n \equiv$ degree of polymerization (unknown)
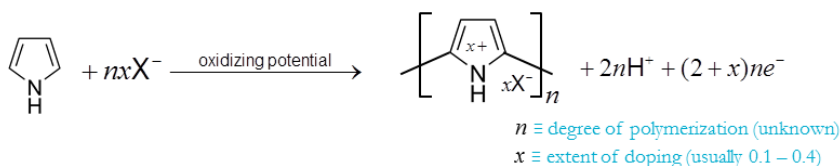$x \equiv$ extent of doping (usually $0.1 - 0.4$)

- Electropolymerization of pyrrole, thiophene, and analogs was performed galvanostatically using a 0.3 M solution of monomer in 1:1 $AlCl_3$:EMIC
- Pyrrole polymerization produces a smooth, robust film that peels off the surface
- Other monomers formed solid, adherent films but did not peel off the substrate
- All experiments performed in glove box (chloroaluminate ionic liquids are air- and water-sensitive!)
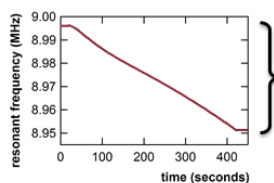

Mass data suggest that $AlCl_4^-$ is the dominant anion dopant after polymerization.

8

Sample Prep: Electropolymerization

- Pyrrole and other conjugated monomers can be polymerized easily via electrochemical oxidation

$$\text{pyrrole} + nx\text{X}^- \xrightarrow{\text{oxidizing potential}} \left[\text{polypyrrole}^{x+} \cdot x\text{X}^- \right]_n + 2n\text{H}^+ + (2+x)ne^-$$

$n \equiv$ degree of polymerization (unknown)
$x \equiv$ extent of doping (usually $0.1 - 0.4$)

Electrochemical Quartz Crystal Microbalance

Change in frequency during polymerization used to calculate mass of deposited polymer film with the Sauerbrey equation
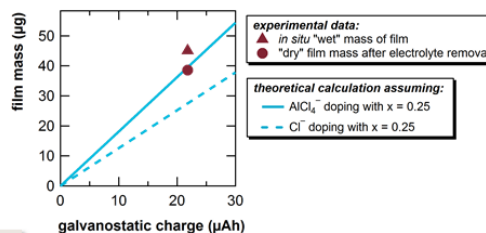

Experimental Conditions:
- Galvanostatic electropolymerization: 1 mA cm^{-2} for 400 seconds
- Electrolyte: 0.3 M monomer in 1:1 (mole:mole) $AlCl_3$:EMI
- Platinum working electrode, aluminum reference and counter electrodes

Calculated cycling capacity of system with polypyrrole at this doping level is **33 mAh g^{-1}**.

9

Polypyrrole Film Characterization
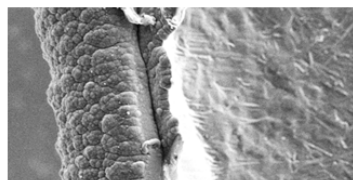
Attenuated Total Reflectance FTIR
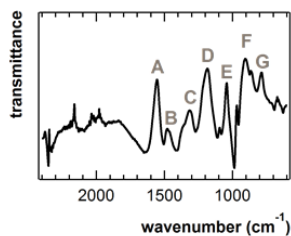
Prominent peaks below 1700 cm^{-1} match published data for doped polypyrrole electropolymerized in organic solvents.

SEM & Energy Dispersive X-ray

100 µm

Energy dispersive x-ray spectroscopy shows presence of elemental aluminum and chlorine in all electropolymerized films (polypyrrole, polythiophene, and analogs).

| Peak	Approximate assignment*	Reported here (doped with AlCl$_4^-$)	From ref.** (doped with ClO$_4^-$)	From ref.** (undoped)
A	C-C & C=C stretch	1550 cm^{-1}	1550	1530
B	C-N stretch	1480	1470	1440
C	C-H & N-H def.	1310	1300	1300
D	C-N str. & C-H def.	1180	1180	1240
E	C-H deformation	1040	1000	1050
F	?	910	900	960
G	?	790	780	750

*B. Tian & G. Zerbi, *J. Chem. Phys.* **92**: 3886 (1990)

**G. B. Street, in *Handbook of Conducting Polymers*, ed. T. A. Skotheim, Vol. 1, p. 280 (1986)

10

Polymer Electrode Redox Behavior

Cyclic Voltammetry at 10 mV s^{-1} of Polymers in Chloroaluminate Ionic Liquids
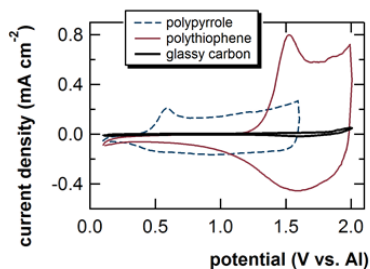
Polythiophene has redox peak-pair at higher potential than polypyrrole (observed previously in other electrolyte solutions).
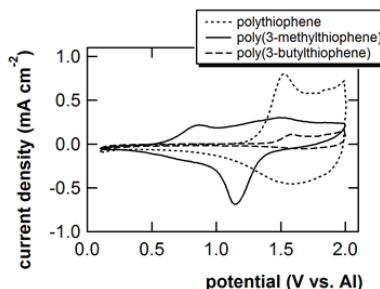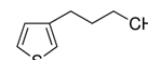
thiophene   3-methylthiophene   3-butylthiophene

Experimental Conditions:
- All polymer films formed galvanostatically on glassy carbon: 1 mA cm^{-2} for 400 seconds in solution of 0.3 M monomer in 1:1 (mole:mole) AlCl$_3$:EMIC
- Cyclic voltammetry performed in 1.5:1 (mole:mole) AlCl$_3$:EMIC at room temperature with aluminum metal counter and reference electrodes

11

Polymer Electrode Redox Behavior

Sandia National Laboratories

Halide Substitution: Cyclic Voltammetry of Polymer Films at 10 mV/s

Halide substitution on thiophene monomer shifts the redox potential of the corresponding polymer to higher values (due to the electron-withdrawing character of the halides).
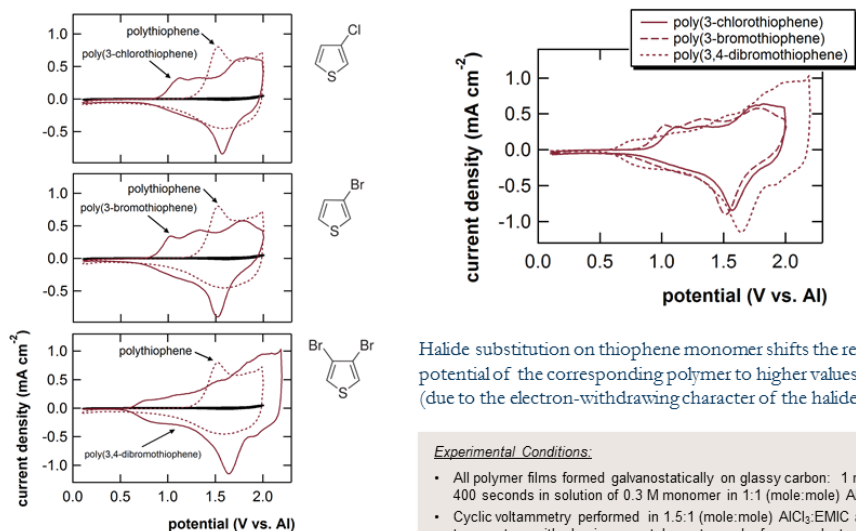
Experimental Conditions:
- All polymer films formed galvanostatically on glassy carbon: 1 mA cm^{-2} for 400 seconds in solution of 0.3 M monomer in 1:1 (mole:mole) AlCl$_3$:EMIC
- Cyclic voltammetry performed in 1.5:1 (mole:mole) AlCl$_3$:EMIC at room temperature with aluminum metal counter and reference electrodes

---

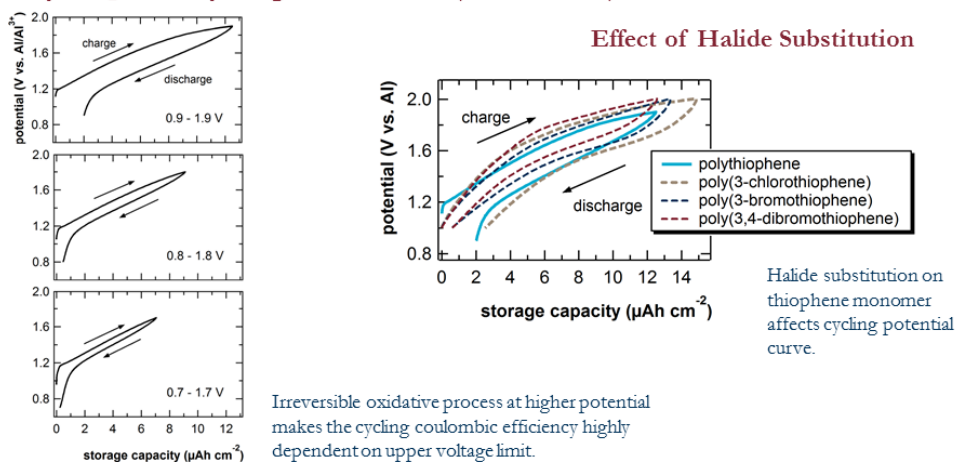# Galvanostatic Cycling

Sandia National Laboratories

Polythiophene Cycling at 10 µA cm^{-2} (1C – 2C rate)

Effect of Halide Substitution

Halide substitution on thiophene monomer affects cycling potential curve.

Irreversible oxidative process at higher potential makes the cycling coulombic efficiency highly dependent on upper voltage limit.

Experimental Conditions:
- All polymer films formed galvanostatically on glassy carbon: 1 mA cm^{-2} for 400 seconds in solution of 0.3 M monomer in 1:1 molar AlCl$_3$:EMIC
- Galvanostatic cycling performed in excess of 1.5:1 (mole:mole) AlCl$_3$:EMIC at room temp. with aluminum metal counter and reference electrodes

13

43

Galvanostatic Cycling

Polythiophene Cycling at 10 μA cm^{-2} (1C – 2C rate)

Effect of voltage range
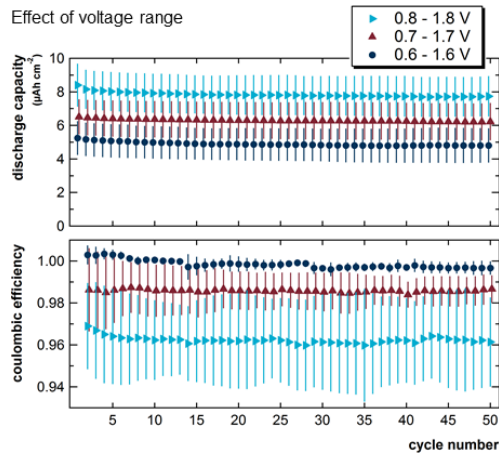
	0.8 - 1.8 V
	0.7 - 1.7 V
	0.6 - 1.6 V

Effect of Halide Substitution

Voltage range: 0.8 – 1.8 V
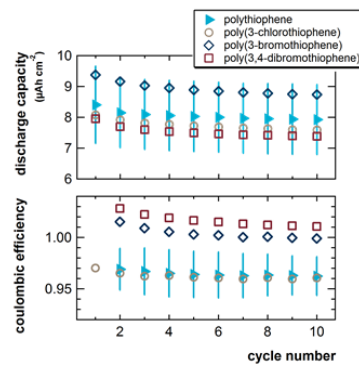
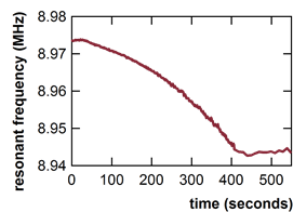| | polythiophene |
	poly(3-chlorothiophene)
	poly(3-bromothiophene)
	poly(3,4-dibromothiophene)

Experimental Conditions:
- All polymer films formed galvanostatically on glassy carbon: 1 mA cm^{-2} for 400 seconds in solution of 0.3 M monomer in 1:1 molar AlCl$_3$:EMIC
- Galvanostatic cycling performed in excess of 1.5:1 (mole:mole) AlCl$_3$:EMIC at room temp. with aluminum metal counter and reference electrodes
- Markers and error bars are the average and standard deviations, respectively, of three experiments.

14

Gravimetric Energy Density

QCM: Convert Area-Specific Capacity of Polythiophene to Gravimetric Capacity


QCM frequency measurement during thiophene electropolymerization shows inefficient polymerization.

Ex situ frequency shift used with Sauerbrey equation to calculate deposited mass

0.14 mg cm^{-2} deposited for a 400-second thiophene polymerization at 1 mA cm^{-2}
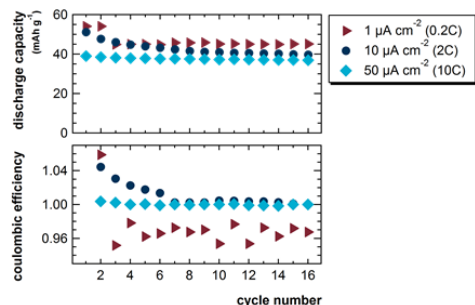
| | 0.8 - 1.8 V |
| | 0.6 - 1.6 V |

- Capacity on plot is specific to doped polymer mass
- Corresponds to doping level of 0.27 (one anion per 3.7 thiophenes)
- Accounting for mass of electrolyte and aluminum metal electrode, effective capacity is 30 mAh g^{-1}
- Specific energy density: 50 Wh kg^{-1}
  - Competitive with flow batteries, lead-acid batteries, and other systems for grid-scale storage
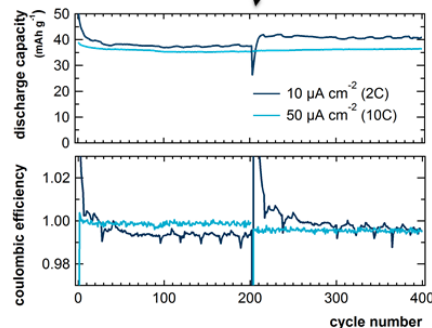
15

44
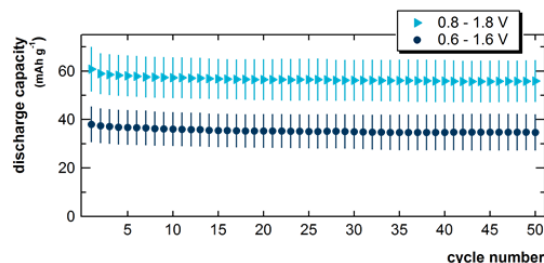
Rate Capability & Long-Term Cycling

Polythiophene Cycling Performance at Various Rates

Pause in cycling: electrode was removed from electrolyte and stored in glove box for 4 months before cycling was resumed.

Large changes in cycling rate resulted in small effect on capacity. The lowest rate tested (0.2C) produced increased capacity but lower coulombic efficiency.

Experimental Conditions:
- All polymer films formed galvanostatically on glassy carbon: 1 mA cm^{-2} for 400 seconds in solution of 0.3 M monomer in 1:1 molar AlCl$_3$:EMIC
- Galvanostatic cycling performed in excess of 1.5:1 (mole:mole) AlCl$_3$:EMIC at room temp. with aluminum metal counter and reference electrodes
- Voltage range for cycling: 0.6 – 1.6 V

16

Conclusions and Acknowledgements

- Cycling of rechargeable aluminum batteries at room temperature with chloroaluminate ionic liquid electrolyte demonstrated
    - Conductive polymers (polythiophene and analogs) as active materials for the positive electrode
    - Aluminum metal as negative electrode
- Electrochemically synthesized polymer films used for initial demonstration
- Energy density of ~50 Wh kg^{-1} is competitive for stationary storage applications
- Steady capacity maintained for at least 400 cycles at 2C and 10C rates

- Acknowledgements
    - Bonnie McKenzie, Sandia National Laboratories (SEM & EDS)
    - Tom Wunsch, Sandia National Laboratories (manager of Advanced Power Sources R&D department)
    - *Funding*: Laboratory Directed Research & Development (LDRD) program at Sandia National Laboratories

17

45

DISTRIBUTION

1	MS0359	D. Chavez, LDRD Office	7911
1	MS0613	Tom Wunsch	2546
1	MS0613	David Ingersoll	2546
1	MS0899	Technical Library	9536 (electronic copy)

Sandia National Laboratories